

Analysis of Steady Multiphase Flow in Porous Media

Across a Hypothetical 2D Percolating Network

Jorijn Holstvoogd (4577493)
Bachelor End Project (AESB3400) – 15th of January 2020
Thesis supervisor: Prof. dr. ir. W.R. Rossen

Abstract

Steady multiphase flow in two-dimensional (2D) porous media has not been established without the continuous fluctuation in pore occupancy. Cox (2019) proves the ability of liquid to bridge a gas-filled pore throat that is narrow and deeply etched, allowing liquid and gas to flow simultaneously. In this investigation, a pore network study was done to discuss the feasibility of steady two-phase flow given the possibility of liquid bridging. Hypothetical percolating gas networks near the percolation threshold were made using Excel and MATLAB to highlight how each established phase can progress through a 2D square lattice. The percolating network describes the gas phase after it has established continuous flow through a water saturated medium. It was found that flow for both phases is easiest near the percolation threshold, where water progresses through a set of isolated clusters and gas has one major cluster that spans the entire lattice. It is predicted that liquid bridging is most problematic near or in the primary gas backbone due to lamellae mobilization. For a larger lattice, it was found that there is more distance between the primary gas backbone and the main water path. In contrast, the possibility of lamellae division occurring due to pressure differences within the lattice is highlighted.

Preface

This report is written for researchers studying microfluidic behavior in porous media to bridge the knowledge of microscopic multiphase flow to their behavior through a pore network. Pre-requisite knowledge of percolation theory, foam generation mechanisms and basic programming is recommended. This research focuses on determining the feasibility of multiphase flow in 2D porous media. This is done by highlighting possible flow paths for two phases in a percolating square network and discusses the problematic scenarios that can arise within this network.

Furthermore, I would like to show my gratitude to Prof. W.R. Rossen for his support and supervision throughout the course of this investigation.

Delft, 15 January 2020,
Jorijn Holstvoogd

Table of Contents

| | |
|---|----|
| Abstract..... | 1 |
| Preface | 1 |
| Symbols and Color Legend | 4 |
| Symbols..... | 4 |
| Color Legend | 4 |
| 1. Introduction | 5 |
| 2. Theory | 7 |
| 2.1 Percolation Theory..... | 7 |
| 2.1.1 Percolation Theory in Reservoir Geology | 7 |
| 2.1.2 The Basics of Percolation Theory | 7 |
| 2.1.3 Variants of Percolation | 8 |
| 2.1.4 Bond Probability and Pore Throat Size | 8 |
| 2.1.5 Randomness of Percolation..... | 8 |
| 2.2 The Pore Space | 8 |
| 2.2.1 Time Frame..... | 8 |
| 2.2.2 Geometry of the Lattice | 9 |
| 2.2.3 Isolated Clusters | 9 |
| 2.2.4 Primary and Non-Primary Gas Backbone | 10 |
| 2.3 Flow..... | 10 |
| 2.3.1 Gas Flow | 10 |
| 2.3.2 Water Flow | 11 |
| 2.4 Capillary Mechanisms | 12 |
| 2.4.1 Lamella-generation Mechanisms | 12 |
| 2.4.2 Stabilized Liquid Bridging and Snap-Off | 14 |
| 2.5 Conductivity of Multiphase Flow | 16 |
| 2.5.1 Conductivity..... | 16 |
| 3. Methodology..... | 17 |
| 3.1 Excel Method | 17 |
| 3.2 MATLAB Method..... | 18 |
| 3.3 Excel Method vs MATLAB Method | 18 |
| 4. Results | 20 |
| 4.1 Excel pore space 16x16 statistics | 20 |
| 4.1.1 Gas Conductivity..... | 20 |
| 4.1.2 Water Conductivity..... | 20 |
| 4.2 Excel pore space 32x32 statistics | 22 |
| 4.2.1 Gas Conductivity..... | 22 |
| 4.2.2 Water Conductivity..... | 22 |
| 4.3 MATLAB Results | 23 |
| 4.4 Flow Observations | 25 |
| 4.4.1 Gas Flow Trend..... | 25 |
| 4.4.2 Water Flow Trend..... | 26 |
| 4.4.3 Water and Gas Flow | 26 |









| | |
|---|----|
| 4.4.4 Problematic Flow Scenarios | 26 |
| 4.4.5 Additional Water Flow Paths..... | 27 |
| 4.5 Observed Lamellae Generation Mechanisms | 27 |
| 4.5.1 Leave Behind | 27 |
| 4.5.2 Lamella Division..... | 27 |
| 5. Conclusions | 28 |
| 6. Discussion..... | 29 |
| 6.1 Modeling of the Gas and Water Paths..... | 29 |
| 6.2 Further Research and Considerations..... | 29 |
| 6.2.1 Feasibility of Liquid Bridges | 29 |
| 6.2.2 Volume Progression Through Liquid Bridges..... | 29 |
| 6.2.3 Lamella Division Across Dangling Ends..... | 29 |
| 7. References | 30 |
| Appendices..... | 32 |
| Appendix A – Excel Results: Pore Space 16 x 16 | 32 |
| Appendix B – Excel Results: Pore Space 32 x 32 | 34 |
| Appendix C – MATLAB Results: Bond Percolation and Lattice for p:0.45-0.55 | 35 |
| Appendix D – MATLAB Script: Bond Percolation and Lattice for p:0.45-0.55 | 38 |
| Appendix E – MATLAB Script: Percolation Statistics for p:0.40-0.60 | 43 |
| Appendix F – MATLAB Script: Dijkstra’s Shortest Path Algorithm | 48 |

Symbols and Color Legend

Symbols

| Symbol | Description |
|--------|----------------------|
| p | Occupation threshold |
| p_i | Bond probability |
| r_i | Pore throat radius |

Color Legend

| | |
|---|--------------------------|
|  | Pore pillars |
|  | Open pore |
|  | Closed pore |
|  | Isolated cluster |
|  | Non-primary gas backbone |
|  | Primary gas backbone |
|  | Liquid bridging |
|  | Liquid pathway |

These colors and textures are used throughout the investigation in the shown Figures.

1. Introduction

Microfluidics refers to the behavior and the manipulation of fluids that are constrained to a small geometric pore space of a microfluidic device (Fallahi et al., 2019). This device can consist of a two-dimensional (2D) network etched into a glass or silicon chip. In this constrained geometry, as in geological pore networks, capillary action governs mass transport. Understanding microfluidic behavior can help us manipulate it to represent a wide range of modern-day applications (Lifton, 2016). These applications include enhanced oil recovery, which is the focus setting of this study.

In microfluidics, the pore space governs how fluids flow across a given network through capillary interactions. Therefore, the geometry of the individual pores and the connectivity of the network is of essence in understanding how a fluid can penetrate a pore space. Conventional microfluidic devices use 2D networks of pores. In a 2D network, percolation theory says that two phases cannot both form long connected pathways for flow; flow is possible only if the phases alternate occupancy of pores or pore connections (pore throats) (Larson et al., 1981). Alternating occupancy of pore throats is called snap-off (Rossen, 1996), and leads to the creation of foam. If simultaneous flow without fluctuating pore occupancy is not possible, then demonstration of foam generation by snap-off in microfluidic devices (Kovscek et al., 2007) is not a convincing proof of the mechanism for geological porous media.

Foam can be an important tool in enhanced oil recovery, as the physical properties of the foam can shape and alter the flow in porous media. Often a reservoir can be heterogeneous, having various layers differing in permeability, which can obstruct flow for enhanced oil recovery. Gas injected for enhanced oil recovery can remove the remaining oil out of a reservoir where gas sweeps (Lake et al., 2014). However, the sweep efficiency is often poor as a result of the reservoir heterogeneity, viscous instability and gravity override. Foam generation in the reservoir can directly fight the causes of the poor sweep efficiency and improve oil recovery as it controls the gas mobility (Lake et al., 2014). In heterogeneous formations, the foam restricts and reduces mobility in the more-permeable layers to divert the flow to lower-permeability layers. Viscous instability is reduced by the viscous foam that reduces gas mobility. By increasing viscous pressure gradient, foam can also help fight gravity override, where the less-dense fluid flows above of a denser fluid (Rossen & Duijn, 2004) (Shan & Rossen, 2004).

Microfluidic devices are not strictly 2D networks. If the etching is deep and pore throats narrow, liquid can bridge across the top and bottom of a throat while gas flows through the middle of the throat (Cox, 2019). If shown to apply generally, this mechanism re-establishes the possibility of simultaneous two-phase flow in these networks without fluctuating pore occupancy and the relevance of microfluidics to studies of foam generation.

The premise of this study comes from a larger project on steady multiphase flow across a microfluidic network. This project is divided into two parts: 1. the capillary and geometrical conditions for bridging and 2. multiphase flow across a hypothetical 2D network of a porous medium made possible by liquid bridging. This study will focus on the second part of the larger project. Specifically, this thesis addresses the question: What are the geometric conditions of a network that allow steady multiphase flow (without fluctuating pore occupancy) given the possibility of liquid bridging?

In addition, it also addresses the following questions. For a 2D percolating network, for what occupation threshold is gaseous flow possible? How does water flow in the presence of gas flow? What are the lamellae-generation mechanisms that are expected?

This report will start with a brief overview of the necessary concepts needed for the rest of the investigation. Then, the applied methods are discussed and lastly the results are explained, and conclusions are made.

2. Theory

2.1 Percolation Theory

2.1.1 Percolation Theory in Reservoir Geology

Porous media are difficult to define in nature due to the geological uncertainty. This geological uncertainty is due to our lack of knowledge of the precise structure and morphology of the subsurface. Reservoir geologists therefore use several methods to understand the flow of water and hydrocarbons in the subsurface on a macro- and microscopic scale. One of those methods is percolation theory, which aims to describe the morphology and transport through randomly disordered porous media by statistical means (Hunt et al., 2014). Thus, percolation theory is a branch of statistical physics, a model of connectivity that can be applied to describe a porous medium in a certain representative elementary volume (King & Masihi, 2019). By understanding a part of the reservoir on a small scale, other properties can be estimated to describe the general flow through an aquifer or oil reservoir. It is important to realize that this theory relies on the assumption that flow through the reservoir is dominated by the continuity and connectivity of the network of connected clusters of open pores (pores occupied by a given phase) in the sedimentary rock. Understanding the representative elementary volume is key to describe the connected flow paths (King & Masihi, 2019). However, the focus of this investigation is a microscopic porous media in a 2D setting, to forecast the reservoir performance of multiphase flow.

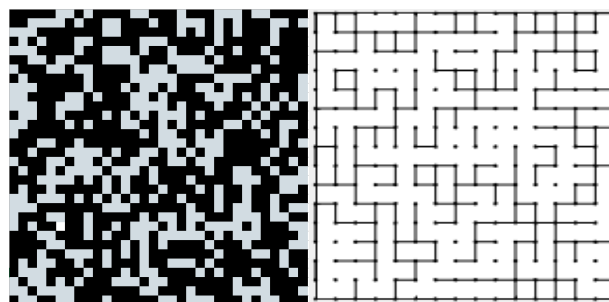
2.1.2 The Basics of Percolation Theory

Percolation across a network depends on the occupation threshold of the system and the bond probability for sites (pore junctions, i.e. pore bodies), and bonds (pore connections, i.e. pore throats) (King & Masihi, 2019). The occupation threshold is the threshold at which a site or bond can be occupied by a given phase. The bond probability is the likelihood that a space is either “open” or “closed”. An “open” site or bond is one that has a bond probability greater than the occupation threshold and therefore could be invaded by the nonwetting phase. A “closed” site or bond is one with a bond probability below the occupation threshold, and could not be invaded. If a site is open, we then consider the probability of flow, whether it is connected to an infinite network of open bonds and sites that could conduct flow over large distances.

Percolation theory analyzes the size of the connected clusters through the occupation threshold by statistical means. The size of the clusters is directly proportional to the increase of the occupation threshold until the percolation threshold, where the percolating system includes at least one large cluster that spans the whole system from one side to the other (Selyakov & Kadet, 1996). The dimensionality and the network type of the infinite or finite-sized system changes the percolation threshold at which the cluster will span across the entire system. In this report we consider the percolation threshold to be defined by the system and has a value of 0.5, while the occupation threshold is a value altered to investigate percolation.

2.1.3 Variants of Percolation

As previously mentioned, percolation is dependent on the dimension and geometry of the medium. There are two methods of percolation: site and bond percolation. The simplest form of percolation is site percolation, where in an infinite lattice of sites every location can either be “open” or “closed” based on a randomly assigned probability and the occupation threshold. Similarly, it is also possible to arrange in



Figures 1&2: Site percolation (black=open sites, grey=closed sites) and bond percolation

bonds instead of sites. Bond percolation can thus also describe a microscopic pore space where grains (pillars) are not participating in the flow of the system and the system is made out of pore throats and bodies. Understanding the type of percolation that could arise for the wetting and non-wetting phase is important in modelling the possible flow paths.

2.1.4 Bond Probability and Pore Throat Size

The bond probability, p_i , of a pore throat is related to the size of the throats (Selyakov & Kadet, 1996) for a certain pore space distribution through the capillary pressure, which determines the ability of nonwetting phase to enter the throat. The larger the pore throat radius, the larger the bond probability becomes for gas to occupy that throat. This investigation assumes a given bond probability distribution for a certain microscopic pore-size distribution. More generally, it can be said that the bond probability for a throat p_i is related to the pore throat radius, r_i :

$$p_i = f(r_i)$$

In particular, p_i increases as r_i increases. This is important to note as this will influence the behavior for the flow of the wetting and non-wetting phase. This study, however, is not concerned with the details of the above equation.

The value of the bond probability is described by a uniform distribution function between 0 and 1. For each case we define an occupation threshold p , such that all throats with $p_i > p$ can be penetrated by gas.

2.1.5 Randomness of Percolation

Percolation is by nature a random statistical analysis (King & Masihi, 2019). Due to its random nature, it is possible to produce systems unable to conduct flow at all. It is possible, especially for high occupation threshold, that there are several large clusters that do not connect to one another by which the lattice is unable to produce a flow path for gas.

2.2 The Pore Space

2.2.1 Time Frame

In this investigation, we assume the pore space is initially saturated with water and the gas has already invaded the pore space to the point where the gas phase is continuous. Thus, the gas will have filled every pore body and throat that is accessible and the water will drain from these pores.

2.2.2 Geometry of the Lattice

As mentioned, the geometry of the lattice is important for the flow and percolation of the system. We consider a square lattice in 2 dimensions where the width of the pore throats is a function of the bond probability. The square lattice is a system where a set of pillars are located in a rectangular array restricting the flow of both gas and water. The coordination number for all pore bodies in this network is four; that is, each pore body is connected to four pore throats. While the coordination number is key, the rectangular shape of the pore bodies and throats used for illustration here is not important to the analysis below.

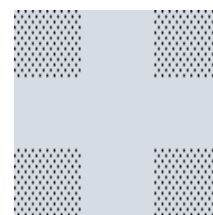


Figure 3:
square lattice

Arrays of 16 by 16 pore bodies are considered, as well as 32 by 32 pore bodies.

To investigate continuous flow, the lattice has wrap-around boundary conditions at the edges of the lattice. If flow is directed to the edge on the right, it can continue its flow on the left side of the lattice. Likewise, if flow is directed to the bottom, it continues on the top.

After percolation the lattice will consist of the three major components,

- Isolated clusters: Open pores that are not occupied by gas because gas does not reach them.
- Primary gas backbone: A network of pores which conducts the most flow. This network includes additional flow paths in the vicinity of the minimum gas path. The minimum gas path represents the shortest path between opposite boundaries.
- Non-primary gas backbone: A network of pores which does not or barely conduct moving gas. This includes the part of the gas backbone that is not the primary gas backbone as well as the dangling ends.

2.2.3 Isolated Clusters

Isolated clusters are areas in the network that are not connected to the conducting cluster of the network. Considering that the investigation focuses on the time frame just after the gas has established continuous flow, the isolated clusters should not be filled with gas, but rather with water and thus should be removed later on in the investigation where possible. Since the wrap-around boundary condition applies, the isolated clusters could be located on the edge of the lattice, where they don't connect on the other side of the lattice. After removing these clusters, the water occupies more pore space, which can be used for an easier water flow path across the lattice. In Figure 4, the isolated clusters are highlighted in orange.

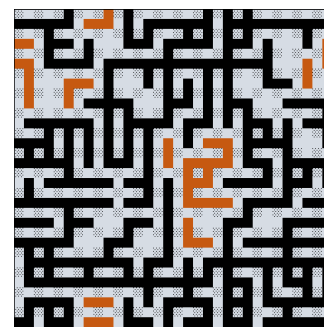


Figure 4: Pore space with
isolated clusters (orange)

2.2.4 Primary and Non-Primary Gas Backbone

The conducting gas backbone is defined as the network in which flowing gas is found. With a larger interconnected pore space network, more pore space will contribute to the flow. However, in this investigation, we focus on flow near the threshold and quantify the resistance of gas flow. Therefore, for simplicity, we define flow in the vicinity of the minimum-length gas path as the *primary gas backbone*. The primary gas backbone is established to allow for a calculation of the resistance, which is very difficult to do for the entire gas backbone. It is possible that some loops are located near the primary gas backbone and do conduct flow, but we assume that this is not as significant as the flow in the primary gas backbone. Since these loops do not conduct most of the moving gas, each loop would have roughly the same pressure as the pores where they connect to the primary gas backbone.

Dangling ends are stagnant bodies of gas which do not contribute to the flow from one side to another. They only have one connection to the backbone, where their pressure is the same as the last pore that is connected to the primary gas backbone.

For simplicity, all the open pores in the network that are not part of the primary conducting gas backbone are labelled as the *non-primary gas backbone*. This includes part of the conducting gas backbone that is not part of the primary conducting gas backbone and the dangling ends.

Note that the non-primary and primary gas backbone should not be confused with the terms dangling ends and conducting gas backbone from literature by King and Masihi (2019). In this literature the gas backbone is defined as the primary and non-primary gas backbones without dangling ends.

2.3 Flow

For both the water and gas flow paths, continuous flow is only established when each phase is able to flow across the lattice. In the primary gas backbone, the path connects to the same pore throat connected through the other side because of the wrap-around boundary condition. Thus, each respective phase has one inlet and one outlet. By doing so, we can approximately evaluate the feasibility of flow of both phases. We assume that both phases have a uniform pressure gradient across the lattice.

2.3.1 Gas Flow

As mentioned previously the gas will enter every accessible pore throat as a function of p , the occupation threshold. As noted, if, for a given throat, $p_i > p$, it is open. If this throat is connected to the primary and non-primary gas backbone, the adjacent pore bodies on either side will also conduct the flow of gas. Isolated clusters in the network are not filled with gas, as gas never entered these clusters to begin with. Furthermore, since the pore bodies are

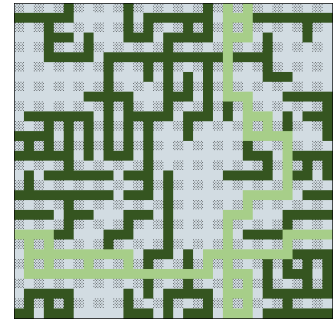


Figure 5: Pore space with highlighted primary gas backbone (light green) and non-primary gas backbone (dark green)

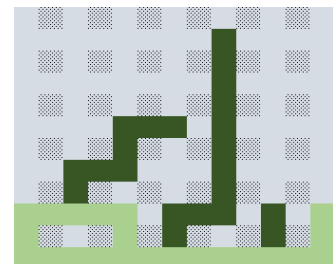


Figure 6: All non-primary pores (dark green) are dangling ends

comparatively much larger than the pore throats, we assume for simplicity that all of the resistance to gas flow is in the pore throats.

The non-wetting phase percolates as a bond-percolation process since pore occupancy is controlled by the throats. The bonds are the pore throats, and this can be used to model the simplest flow path across the lattice.

2.3.2 Water Flow

Before invasion, the lattice was already saturated with water and, thus, after invasion, all the pores that are not filled by gas, contain water. Since pores are etched with uniform depth and vertical walls, water, as wetting phase, continues to occupy the corner regions where pillars meet the upper and lower surfaces of the network (see examples in Figures 9 and 10 below). Water flow across the network is possible if water in these corner regions can interconnect. However, to deduce a general flow path across the lattice the water must cross gas-filled pore bodies. The water can then flow between pore throats through a number of different ways:

- R1: A bent movement where the liquid flow path makes a 90-degree turn around a pillar. During this movement, water flows around a gas-filled pore body. In accordance with liquid bridging, the water will progress along the corners at the ceiling and floor of the pore body filled with gas.
- R2: A movement where the liquid flows along a pillar between throats on either side of the pillar. By doing so, the liquid must travel along two pore bodies and one pore throat filled with gas.
- Rb: Liquid bridging in the pore throats of the network with simultaneous gas flow. It is assumed that the likelihood that the liquid can bridge is greater in narrowest gas-occupied pore throats of the network. In terms of the percolation network this narrowest pore throat is one that has the smallest probability p_i above the occupation threshold p .

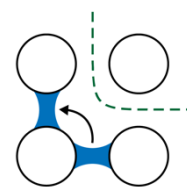


Figure 7: R1 Liquid flow path (blue) with adjacent gas movement (green dotted line)

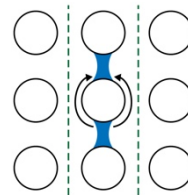
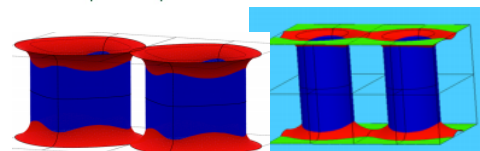


Figure 8: R2 Liquid flow path (blue) with adjacent gas movement (green dotted line)



Figures 9&10: Liquid bridges (Rb) of double channel morphology in red (Cox, 2019)

Due to the existence of isolated clusters, which are to be removed, water can find an easier path through the lattice since pores that already contain liquid barely contribute to the overall resistance of the flow path. We assume that the resistance in corner flow illustrated above is much larger than that through water-filled pores and throats. Thus, if the flow path advances through a pore space already saturated with liquid, no resistance is assigned there.

Since the connectivity of a water flow path through the lattice is not a function simply of bonds or connected sites, the water flow cannot be described using site or bond percolation. However, since the water can progress across the lattice between throats, using the movements described above, a path can be established by observing several lattices. By doing so, remarks can be made on the viability of water flow across an arbitrary lattice with a given occupation threshold.

There are two major assumptions made when deducing the water flow path:

1. The path with the least amount of liquid bridges is preferred.
2. Only the smallest possible pore throats are utilized for liquid bridging.

2.4 Capillary Mechanisms

2.4.1 Lamella-generation Mechanisms

Foam in porous media is defined by the formation of lamellae, surfactant-stabilized water films between bubbles, which in essence define the boundary of the bubbles which make up the foam. A lamella usually takes on a thickness of 30 nm to 100 nm. Ransohoff & Radke (1988) describe the three different lamella-generation mechanisms in porous media through their study of foam in glass bead packs:

- a) “Leave-behind” is a mechanism in which the non-wetting gas phase invades the liquid-saturated pore space and stabilizes liquid films and lenses in the pore throats between gas-occupied pore bodies. By this method of invasion, the gas forms pathways and thereby forms several boundaries in adjacent pore throats. The foam formed by this mechanism, however, is very weak in absence of a surfactant to strengthen the liquid films. Ransohoff & Radke (1998) explain that in a homogenous bead pack, this lamellae creation mechanism was found to be dominating below a critical velocity. The gas percolates through the porous medium in several adjacent pathways in the interconnected pore space. The two gas fronts are not required to occupy the adjacent pores simultaneously. One front can arrive later should capillary pressures rise. It is important to note that this mechanism leaves at least one continuous gas pathway for flow. A major consequence as a result of this mechanism as a whole is that the gas relative permeability of the porous media decreases due to the large number of pathways that have dead-ends or block other pathways. The large number of dead-ends formed can later be used in lamellae mobilization.

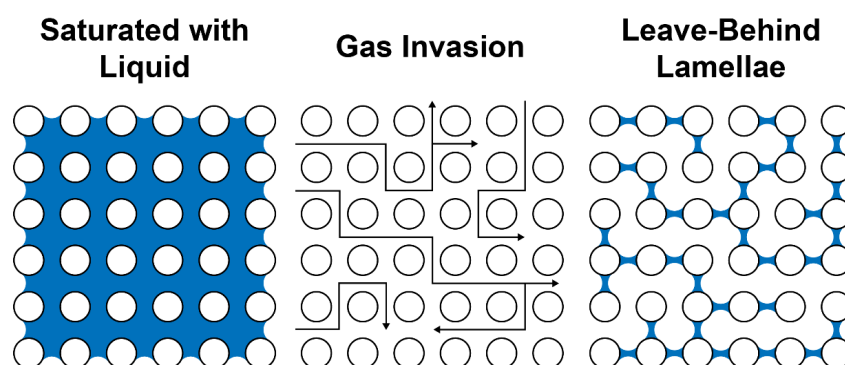


Figure 11: Leave behind mechanism resulting from gas invasion. Based on Rossen (1996).

- b) “Snap-off” is a mechanism in which a gas-bubble penetrates a pore throat (which restricts flow), and later a collar of liquid blocks the pore throat. The resulting liquid lens can later be thinned down to a lamella. This mechanism relies on the temporal variation in capillary pressure. To enter and fill the pore throat, the capillary pressure must

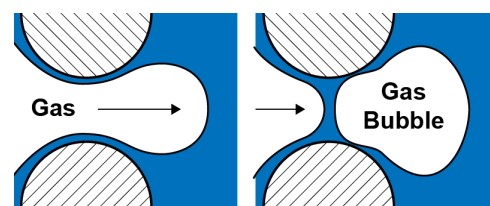


Figure 12: Schematic of Roof snap-off, one of several mechanisms of snap-off Based on Ransohoff & Radke (1998)

first rise to a value at least equal to the capillary entry pressure and then fall to the capillary pressure at which snap-off occurs. Depending on the geometry of the pores, this means that the capillary pressure has to fall to about half of the capillary entry pressure of the pore throat. The difference in the capillary pressure forces the wetting-phase to grow a collar of water in the vicinity of the pore throat and snap-off the throat. The fall in capillary pressure which triggers snap-off for steady flow in homogenous porous media can be explained by any of eight ways (Rossen, 2008), three of which are as follows (Ransohoff & Radke, 1988):

- The mobilized lamellae alter the pressure drop between gas bubbles, causing capillary pressure to fluctuate as foam advances (Rossen, 1990).
- The pressure inside the bubbles is nearly uniform because they are inviscid, while the liquid pressure is reflected by the general flow field and shifting shape of the existing lamellae. Thus, the capillary pressure at the upstream end of long bubbles is much lower than at the downstream (front).
- As the gas penetrates the pore throat into the liquid-filled wide pore body, liquid clearing from the pore body can move back into the throat to cause snap-off. This was discovered by Roof et al. (1970) in their study of oil-trapping in a water-filled porous medium. The premise of this phenomenon depends on the ratio of pore throat to pore body diameters, which allows for water to advance along the pore wall to snap-off the gas bubble at the pore neck. Crucial to the mechanism is that the downstream pore body must be filled with liquid. This mechanism does not apply one the downstream pore is occupied with gas.

Roof Snap-off



Figure 13: Conditions for Roof snap-off illustrated. Based on Rossen (2003)

- The third and final lamellae generation mechanism is lamella division. This mechanism requires mobilizing a lamella to produce more lamellae. However, unlike with the first two mechanisms, some type of lamella creation must have occurred to begin the process of the lamella division. This mechanism creates more lamellae by mobilizing a lamella through a branching point (Rossen, 1996). At the branching point, the lamella can flow into two or more channels; in the process the lamella is split

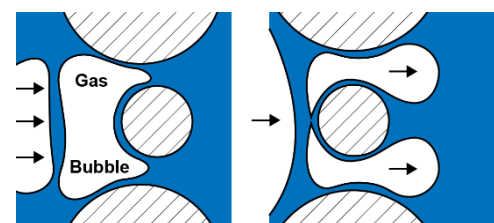


Figure 14: Schematic of lamella division. In this case, lamella division occurs during initial drainage. It can also occur after drainage. Based on Ransohoff & Radke (1998)

into two, one for each channel. If there is only one downstream channel, or other throats are already occupied by liquid, no lamella division occurs. This mechanism depends crucially on having a large enough pressure gradient to start the movement of the stationary lamella to the division point.

2.4.2 Stabilized Liquid Bridging and Snap-Off

To determine a stable flow of simultaneous water and gas, we assume that liquid bridging is possible so that water can flow without the phenomenon of snap-off across gas-filled pores. The capillary pressure conditions for snap-off are already extensively researched; however the conditions for stabilized liquid or capillary bridging for a 2D curved slit are not well known. The following paragraphs summarize some results from the literature on bridging.

In this study, the term liquid bridging is defined differently from most literature studies, such as Broesch & Frechette (2012), Ahmadiouydarab et al. (2015), Moura et al. (2019) and Kusumaatmaja & Lipowsky (2010). In those studies, it is defined as water bridging between two parallel plates. Our definition of liquid bridging is that the liquid connects at the roof or floor of a pore throat. The liquid "bridging" as defined by much of the literature would lead to snap-off in our network by completely blocking the pore throat and not allowing simultaneous gas flow. The liquid bridging we refer to in this study is shown in Figures 9 and 10, where the liquid flow is shown in red. Through this method, the liquid and gas flow can coexist without obstructing gas flow. The first part of the larger study (Cox, 2019) focuses on liquid bridging on a smaller scale rather than an entire network.

As mentioned, this part of the research focusses on the connectivity and feasibility of multi-phase flow in a 2D pore network given that liquid bridging can happen at a microscopic scale. Moura et al. (2019) analyzed the connectivity of a pore network made out of glass beads in which the water invades the air-filled pore space driven by gravity. By doing so, they analyzed how liquid bridges behave across its flow path. These liquid bridges are not located across gas-filled pores and connect between the roof and floor of the pore throats. This is what we consider snap-off. While the system we consider is driven by a given flow velocity and not by gravity, and the liquid morphology differs, remarks are only made about the advancements of liquid bridging in a connecting pore space and the global connectivity of the system. Given that the morphology of the porous medium is favorable for liquid bridging, the water connectivity in the pore space relies heavily on liquid bridging. Furthermore, if snap-off occurs, it crucially impacts the flow of gas. According to Moura et al., at a certain point in time, liquid bridges that are located closer to the inlet are older than those located further along the flow path. Thus, in principle, those liquid bridges have more time to reach a condition favorable for snap-off over bridging. In contrast, in our study we assume a quasi-static process and equal capillary pressure throughout the network. This is of more importance in a larger system, where snap-off events earlier in the network have catastrophic implications on the advancement of gas and thereby restriction of the water flow. Moura et al. (2019) confirms this and mentions that in their experiment, a small number of snap-off events obstructed large clusters of the connecting water flow. While we define snap-off as obstructing gas flow, Moura et al. (2019) defines snap-off as the breaking of liquid films in the pore throats directly obstructing the water flow. They concluded that water transport happens through a connected secondary network of liquid bridges and films. The interruption and rupture of a single entity of this network can regionally disconnect large sections of the

system. Therefore, the stability of liquid bridging plays a large global role in the connectivity and conductivity of the system. Additionally, this study concluded that liquid in trapped regions can be mobilized by liquid bridging and this should be considered when simulating water flow in porous media. While this study offers insights on the connectivity that liquid bridging brings to the system, directional flow phenomena where both phases have a velocity gradient through the network cannot be explained.

For our study, it is also important to consider the consequences of a fluctuating flow throughout the lattice. Ahmadlouydarab et al. (2015) studied the effects of a fluctuating flow in respect to the stability of liquid bridging between two parallel plates. Although this liquid morphology leads to snap-off in our investigation and is not the same as we are considering in this report, it can impose consequences of unsteady flow. While it was mentioned that the stability depends on the wettability of the plates, it was found that for a large externally driven frequency, the bridges remain stable. This case then approaches a stationary setting. Only when the external flow has a very short frequency does the liquid bridge rupture and or detach. It was found that stable flow for significant frequencies was a result of less deformation due to rapid changes in flow direction as well as motion in the contact lines of the substrate. The minimum critical frequency depends on the geometry of the system and fluid properties such as viscosity. In respect to the liquid flow across the hypothetical percolating network, a failure of one bridge could possibly induce a fluctuating flow velocity below the critical frequency and destabilize liquid bridges further along the flow path.

Valencia et al. (2001) analyzed a liquid morphology close to that of what we are considering with wetting layers on the top and bottom of the lyophobic substrate. They show that for a small volume, the liquid channel takes the shape of a cylindrical segment. However, if the volume per unit length is increased to a value greater than $(\pi/8)L^2$, where L is the width of the liquid channel, the channel has a variable cross section along the segment. The largest

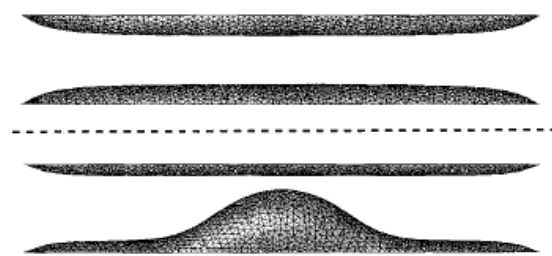


Figure 15: Symmetrical liquid channels, Asymmetric liquid channel with unequal volumes. The bottom channel forms a bulge. (Valencia et al. ,2001)

part of this variable cross-section can be labeled as a 'bulge' which extends into the channel as flat sleeves on either side of the bulge. They concluded that for a small volume of two liquid channels with a symmetrical configuration and similar cross-section, the channels are stable. While for a larger volume of two channels with bulges, the channels are unstable. In this study, they considered a stationary case and did not consider a gas-driven velocity gradient which could possibly interact with the bulges. However, this highlights the importance of a steady small volume and the instability that may arise with larger volumes and unsteady flow.

The steady multiphase flow across the 2D medium relies on the feasibility of liquid bridging without instabilities formed by deformations due to variable volume flow. Ahmadlouydarab et al. (2015) and Valencia et al. (2001) both highlight the importance of steady flow rates in maintaining the stability of liquid bridges. While Moura et al. (2019) states the essence of stable liquid bridging on the connectivity and implications on the general water flow.

2.5 Conductivity of Multiphase Flow

2.5.1 Conductivity

In this investigation, the conductivity of the gas and water is estimated. Given a constant flow velocity of both phases, the conductivity is a measure of the sum of the resistances in the flow paths. For the gas, this is easier to quantify as the resistances of the pore throats or bonds are assumed to be the same, for simplicity. While in reality this is not the case given a pore-size distribution, the resistance of every pore throat is assumed to equal to one. The conductivity for gas can be modelled using an analogy to electrical conductivity where the total resistance can be comprised of resistances in series and in parallel using the following formulae;

$$\text{Series: } R_t = R_1 + R_2 \quad (1)$$

$$\text{Parallel: } R_t = (R_1^{-1} + R_2^{-1})^{-1} \quad (2)$$

Using these formulae for the gas path across a system (the "primary gas backbone" in our terminology) the conductivity is calculated using the following formula;

$$\text{Conductivity: } C = \left(\frac{1}{\sum R}\right) \quad (3)$$

Where R here represents the resistance of one throat. The conductivity of the water is not easily quantifiable since we do not know the resistances of the segments R1, R2, and Rb illustrated in Figures 7 to 10, pending the conclusions of the parallel study of surface configurations and stability of bridges. Since the flow path of water is so constricted in all three of these configurations, we can say that the resistances are large. Therefore, to estimate how easily water flows across the lattice, we will count the number and types of these resistances. As noted above, we neglect the resistance in flow through water-filled pores compared to R1, R2 and Rb. The conductivity of water is estimated in a similar manner as the gas. The higher the sum of the present resistances, the lower the conductivity of the percolating lattice.

Note that the calculated conductivity is based on the primary gas backbone. In reality, the entire gas backbone (primary and non-primary gas backbone without the dangling ends) conduct flow reducing the total resistance and resulting in higher conductivities.

3. Methodology

The aim of the investigation is to highlight several flow paths for the wetting and non-wetting phase in percolating systems with a variable occupation threshold. To create these percolating pore networks, Microsoft Excel and MATLAB were utilized.

3.1 Excel Method

A 16 by 16 pore space was established using pore pillars, throats and bodies. The pore pillars were simply left blank. The pore throats' bond probability p_i was defined by the random function:

$$\text{Rand}()$$

This function returns a random value between 0 and 1 from a uniform distribution. All the p_i values in the network were then subtracted by the occupation threshold, p . If this value was negative, it was corrected to zero and thus it is a closed pore throat. This was done by the following if statement:

$$\text{If}(p_i > p; p_i - p; 0)$$

The pore bodies were defined as a small value, 0.001, if one of the adjacent pore throats are open, using the following if statement:

$$\text{If}(\text{sum}(\text{values of adjacent pore throats}) > 0; 0.001; 0)$$

At the edge of the system, the wrap-around boundary condition is considered by including throats on the other side of the lattice when determining if the pore body is open.

At this point the system is defined, and every cell with a value above zero is an open pore body or throat. If the pore is 0, it is closed and filled with liquid. If the cell contains a blank, it is a pore pillar. Then, these conditions were visualized utilizing color-coding rules, to define pore pillars, closed and open pores as textured grey, grey and black colors, respectively. The percolating network can now be visually observed and analyzed.

Since at this point, the lattice still contains several clusters of isolated gas pores, these are visually assessed and removed by changing the value of the cell from an arbitrary bond probability to zero.

For a given occupation threshold, the shortest gas path is assessed visually in all possible directions (top to bottom, left to right). The same is done with the water path. For the gas path, the sum of the resistances is calculated for a flow in the primary gas backbone and the conductivity is determined.

For the water, the minimum flow path is deduced much like the gas path. However, if the liquid has to bridge a gas-filled pore throat, the gas-occupied throat with the smallest (nonzero) value of $(p_i - p)$ is determined. This throat is among the narrowest entered by gas, which makes it most likely to sustain stable liquid bridging. By summing the resistances of the individual liquid segments (including those illustrated by Figures 6 and 7 above), the most likely flow path can be assessed. This path is one which is that with the fewest segments R1 and R2 and liquid bridges.

This process is repeated for an occupation threshold range of 0.48-0.52 as well as for a larger lattice of 32 by 32 pores with an occupation threshold range of 0.49-0.51.

3.2 MATLAB Method

Two MATLAB scripts were written to describe the minimum gas path for a given percolating system and describe the randomness of percolating systems by a large set of iterative calculations. Unfortunately, these scripts are unable to devise the minimum water path, as they are unable to remove isolated clusters since the algorithms cannot deduce if a section is part of the largest cluster in the network. However, since gas percolates as bond percolation, the system can be defined in a series of nodes and bonds which are the pore bodies and throats respectively. Dijkstra's shortest-path algorithm (Kirk, 2006) is utilized to find the shortest path for a given percolating network. In this algorithm, the nodes have defined coordinates, and bonds are defined by connections between nodes. By defining open-pore throats as bonds between nodes, connections can be established. Four different types of nodes have to be defined: left to right inner nodes, top to bottom inner nodes, left boundary condition and the top boundary condition. For flow in the horizontal direction, it was said that only the connections of the inner and top boundary nodes are relevant. Likewise, for flow in the vertical direction, only connections of the inner and left boundary nodes are considered.

Finally, in the first script, the shortest flowing path for occupation thresholds ranging 0.45 to 0.55 was illustrated along with their original lattice form. 5 iterations were made for each occupation threshold. The results of the first script can be found in appendix C and the script itself in appendix D. The gas path in the vertical direction is shown in blue, while the gas path in horizontal direction is highlighted in red. If a boundary condition is used, there will be a straight line across the lattice.

The second script determines how many times an arbitrary lattice displays gas conductivity for a hundred iterations for every occupation threshold ranging from 0.40 to 0.60. Four different quantities were calculated for each occupation threshold:

- The number of flowing systems if there is any flow
- The number of flowing systems in the horizontal direction
- The number of flowing systems in the vertical direction
- The number of flowing systems with horizontal and vertical flow

This script can be found in appendix E.

3.3 Excel Method vs MATLAB Method

While both methods can be utilized to make conclusions about a 2D percolating network, each method has its advantages and disadvantages. The Excel method easily defines and displays the percolating network, which can be edited to remove any isolated clusters and to highlight the gas and water flow paths. However, the lattices chosen always have flowing gas paths in at least one direction, which by the nature of percolation is not always the case. The MATLAB method can define the percolation network for a large variety of occupation thresholds and iterations. By doing so, the scripts can objectively show the nature of percolating systems for a large number of iterations. However, since they are unable to recognize if an arbitrary pore is part of the largest presented cluster, they cannot remove the isolated clusters. These isolated clusters are of essence in describing the water flow across the lattice.

When deducing the conductivities of the water and gas pathways, Excel can quantify the amount of individual liquid movement segments and calculate the gas resistance to flow by resistances in parallel. The MATLAB method however, is unable to assess which pathways are significant enough to contribute to flow and calculate the resistance in parallel.

4. Results

4.1 Excel pore space 16x16 statistics

4.1.1 Gas Conductivity

For nine lattices with occupation threshold ranging from 0.48 to 0.52, the gas conductivities were calculated. The first five lattices ranging from 0.48 to 0.50 have flow occurring in both directions (vertical and horizontal). However, only the conductivity of the most conductive primary gas backbone of the two directions for each lattice was shown below in Figure 16.

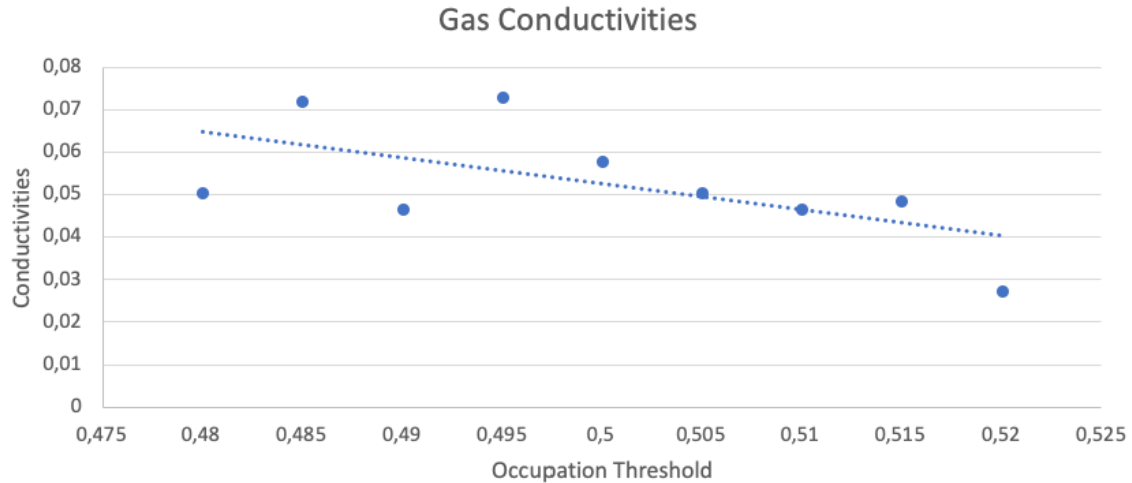


Figure 16: Gas conductivities for occupation threshold ranging 0.48-0.52 for a 16x16 lattice

The total resistance of the primary gas backbone can be lower than a single direct minimum path across the lattice due to flow diverting into several side streams. Note that according to formula 2, the resistances of sections of the primary gas backbone can be modeled by resistance in parallel. The likelihood that the primary gas backbone can divert into several parallel streams is higher when the network is more connected with a lower occupation threshold.

While there is a general trend of a decrease in conductivity with an increase in occupation threshold, the nature of percolation remains random. As a result, even some lattices with a low occupation threshold display a reduced conductivity such as the lattice with occupation threshold 0.490.

4.1.2 Water Conductivity

For the water flow paths, we can't deduce the conductivity as the resistances of the different types of water flow have not been concluded. Therefore, only the amount of times the three different movements were present in a given flow path was determined. As mentioned, these flow paths were made with the assumption that the most ideal flow path is one that is the shortest and has the least number of liquid bridges. Using liquid movements, R1 and R2, the section of the path that doesn't require bridging can be modelled. The sum of R1 and R2 and the number of liquid bridges (Rb) was determined and shown in Figure 17.

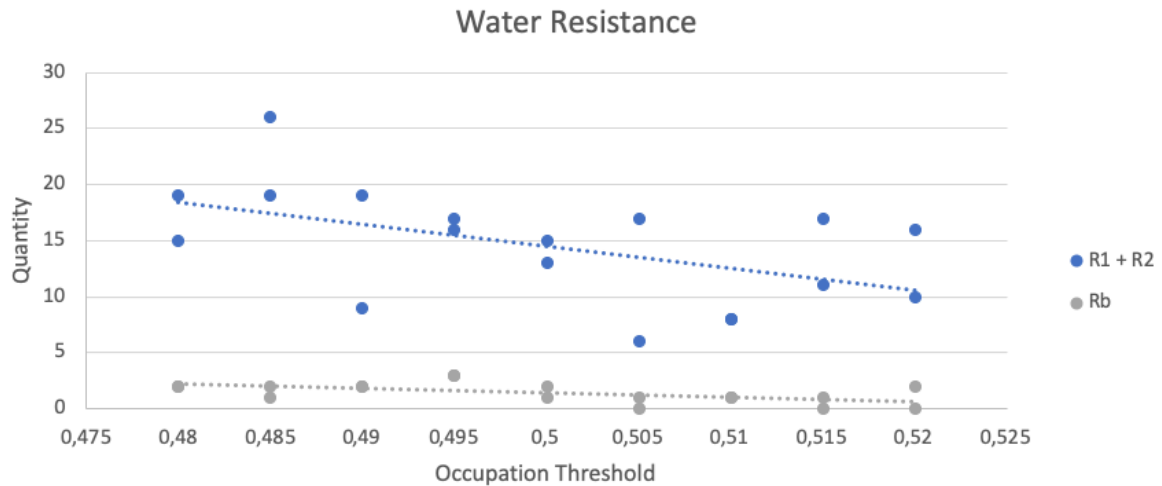


Figure 17: Elements in water resistance for occupation threshold ranging 0.48-0.52 for a 16x16 lattice

As expected, an increase in the occupation threshold results in a flow path with less overall resistance for water. This can be concluded from the two receding trendlines. Most likely this is due to the decrease in connectivity of the percolating network of the gas phase and increase in the size and number of isolated clusters, in which the water can advance through without significant resistance. Since the conductivity is inversely proportional to the sum of the resistances, the conductivity of the water phases increases with increasing occupation threshold.

It was stated that liquid bridging was most feasible in pore throats that are among the smallest in the network (Cox, 2019). Thus, the smallest pore throats were chosen for liquid bridging. The size of the pore throats inhibiting liquid bridges are based on how much they exceed the occupation threshold as illustrated in Figure 18.

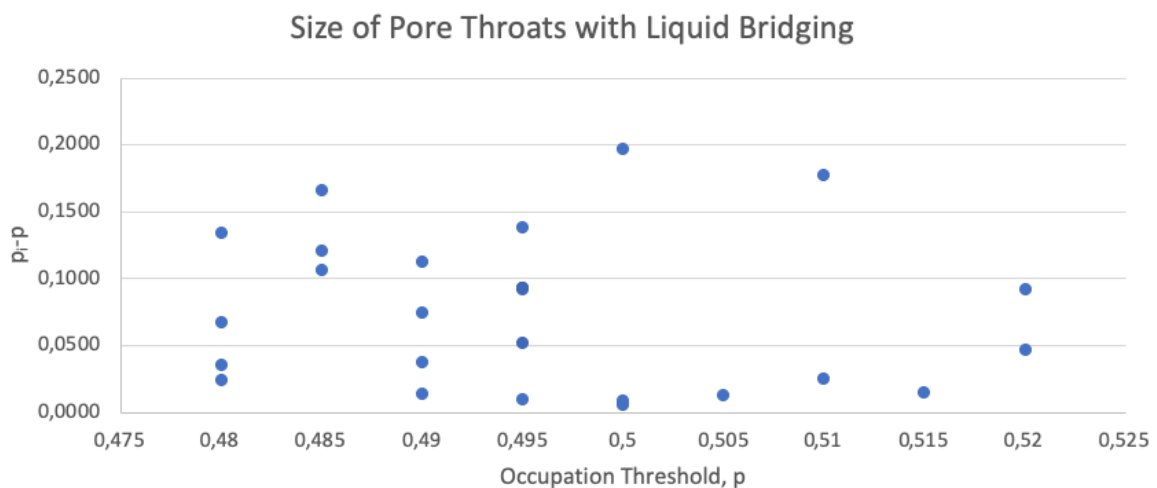


Figure 18: Size of pore throats with liquid bridging for occupation threshold ranging 0.48-0.52 for a 16x16 lattice

In general, a liquid pathway can cross a gas-filled pore that is relatively small compared to the largest pore throat in the network. However, given that the liquid prefers flow through the fewest bridges, it is in some cases impossible to find the narrowest pore throat. The lattices with occupation threshold 0.5 and 0.51 display this behavior, where their respective flow

paths have to cross a pore throat that is quite significant. For a more direct path, the liquid is forced to bridge in more locations given that a small pore throat is in the proximity of this most direct path.

4.2 Excel pore space 32x32 statistics

4.2.1 Gas Conductivity

Likewise, for the larger pore space of 32 by 32 pores, the gas conductivities across the lattice were calculated. This lattice is four times the size of the smaller lattice. The conductivities were calculated for three different lattices with occupation threshold ranging from 0.49 to 0.51. These occupation thresholds were chosen to analyze conductivities near the percolation threshold.

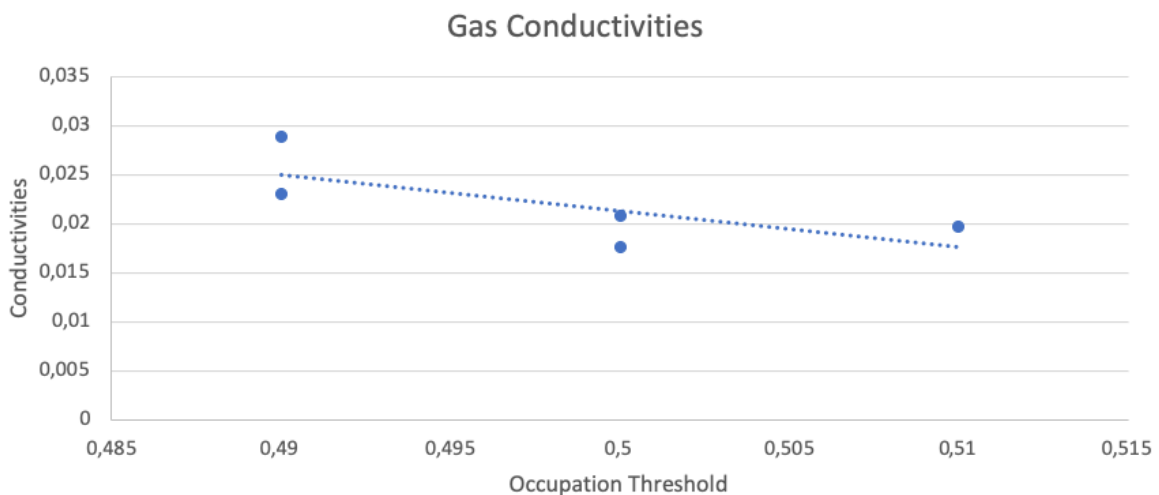


Figure 19: Gas conductivities for occupation threshold ranging 0.49-0.51 for a 32x32 lattice

Alike the smaller lattice, the conductivity tends to decrease with increasing occupation threshold. The first two lattices with occupation threshold 0.49 and 0.5 have flow in both directions while the final lattice of occupation threshold 0.51 has only flow in one direction. This is the same pattern observed in the smaller lattices and thus this trend is independent of the size of the lattice.

4.2.2 Water Conductivity

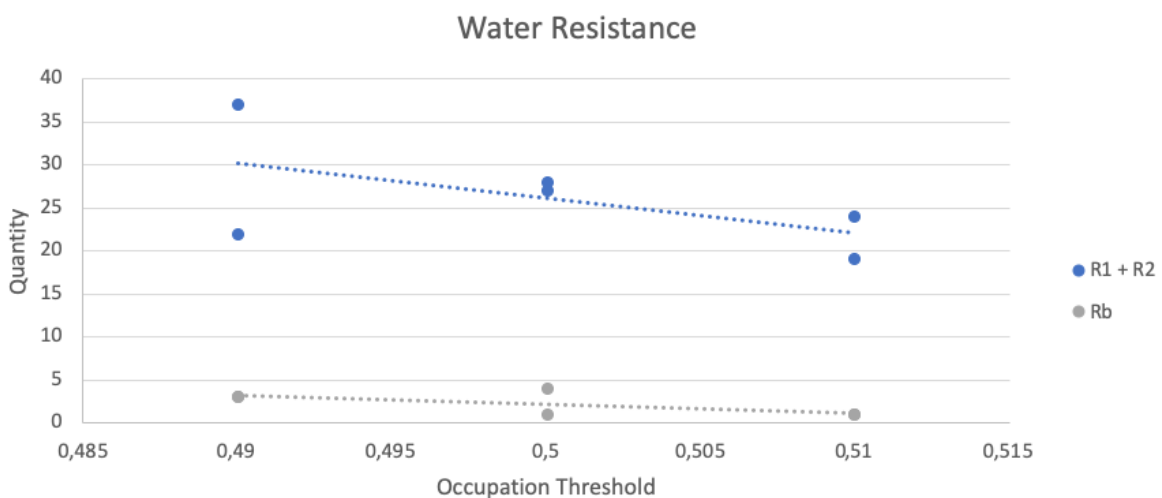


Figure 20: Gas conductivities for occupation threshold ranging 0.49-0.51 for a 32x32 lattice

Since the pathways to cross the lattice are twice as large than the smaller lattice, the water path requires more water movements. Also, the trend of more conducting pathways of water flow with a higher occupation threshold found in Figure 17 still holds in Figure 20. This is again concluded by the receding trendline of the resistances of liquid movements.

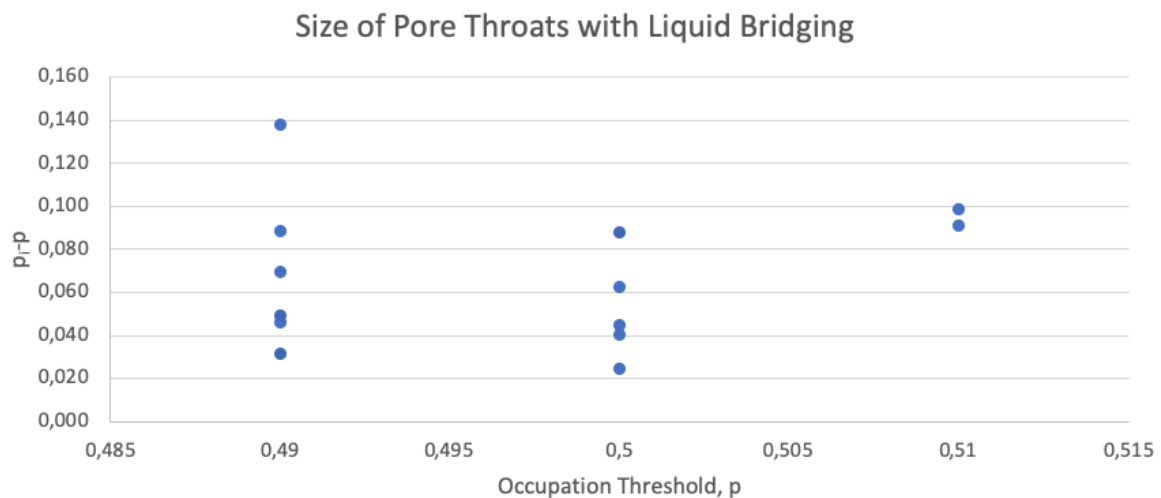


Figure 21: Size of pore throats with liquid bridging for occupation threshold ranging 0.49-0.51 for a 32x32 lattice

While the size of the lattice is increased, the probable path the liquid takes is not any more favorable than in the smaller lattice. This is because the liquid pathway already aims to flow across the smallest possible pore throat for bridging.

What is noticeable from Figure 21 and also visible in Figure 18, is the decrease in required liquid bridging with lattices of greater occupation threshold.

4.3 MATLAB Results

The main purpose of utilizing a MATLAB script was to study gas percolation and the randomness of percolation as a function of the occupation threshold. Results of occupation threshold ranging from 0.45 to 0.55 are shown in appendix C. The red paths display the horizontal gas flow and the blue paths show the vertical gas flow.

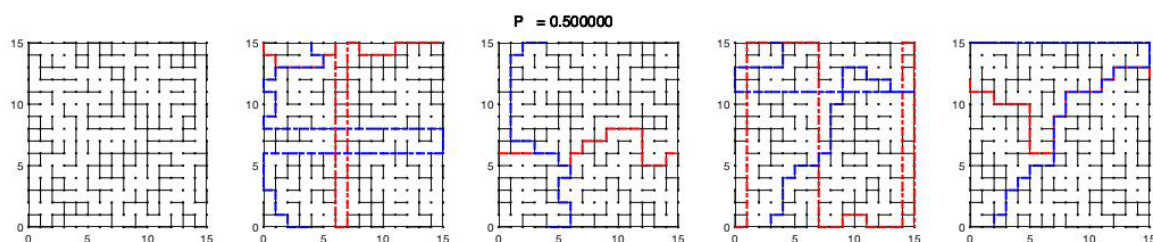


Figure 22: Bond percolation of gas flow for p:0.5 of a 16x16 lattice

The most noticeable distinction from the Excel method is that not every lattice before or at $p=0.5$ shows gas percolating in both directions. Some lattices such as the first lattice in Figure 22 do not percolate in any direction. This can be problematic if you consider only one inlet and outlet. Alike the results found by using the Excel method for highlighting flow paths, the likelihood that gas percolates in any direction decreases with a higher occupation threshold. To validate this, the quantity of percolating systems was calculated for a hundred iterations for occupation threshold ranging from 0.40 to 0.60 in Figure 23.

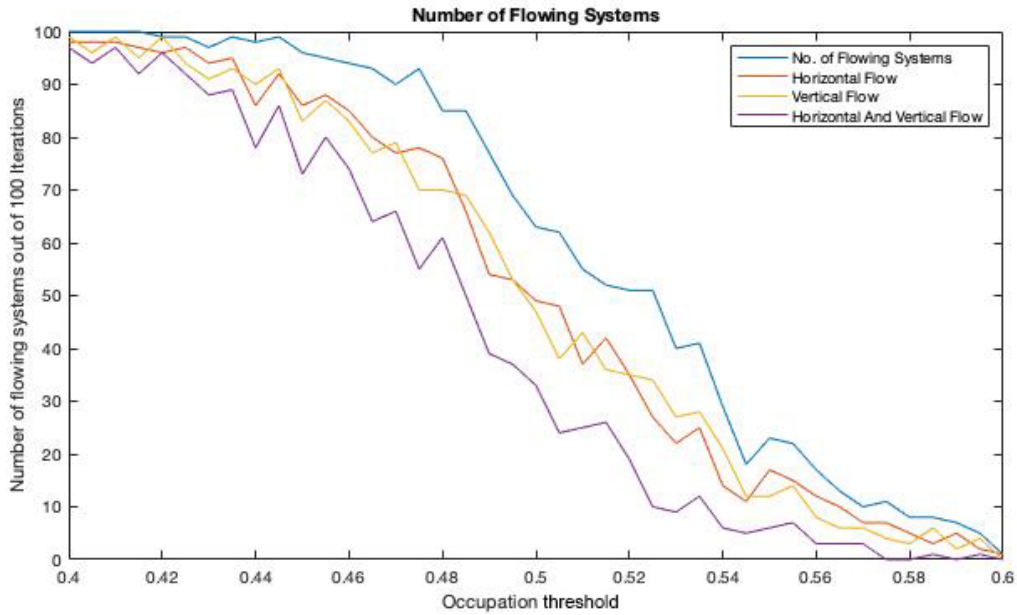


Figure 23: Number of flowing systems for 100 iterations of $p:0.40-0.60$ of a 16×16 lattice

As expected, the quantity of flowing systems decreases sharply just before the percolation threshold of 0.5. At this percolation threshold, the number of flowing systems that conduct flow in at least one direction is just above half of the iterated systems. This shows that percolation for only one inlet and one outlet is restricted. The quantity for which flow is guaranteed in both directions for the percolation threshold is just above 30% of all flowing systems. Only at occupation threshold of 0.415, was flow in at least one direction guaranteed. For none of the chosen occupation thresholds is flow guaranteed in both directions.

At the percolation threshold of 0.5, statistically more than half of the bonds in the network are open allowing the flow of gas. However, in some systems, the global connectivity is determined by only a few bonds connecting several smaller clusters to the main cluster. Increasing the occupation threshold decreases the statistical chance of a global connected network. This can explain the decrease in flowing systems in Figure 23.

The average resistance of the minimum gas path was also calculated. This is not to be confused with the primary gas backbone, as this is only considering the shortest path and not small loops found in the primary gas backbone that also conduct flow.

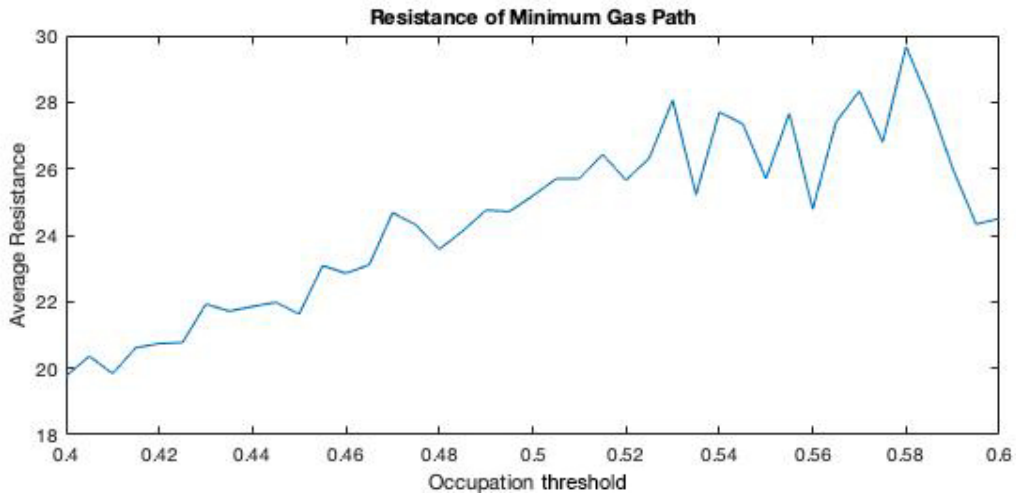


Figure 24: Average resistance of minimum gas path for $p:0.40-0.60$ for a 16×16 lattice

As observed in Figure 24, the resistance of the minimum gas path increases roughly until $p:0.53$. After which the average resistance starts alternating around a value of 27. In actuality considering that the primary gas backbone is larger with higher connectivity, the average resistance of the gas path will be much lower for lower occupation thresholds. While at higher occupational thresholds, the primary gas backbone should conform to the minimum gas path due to reduced connectivity.

4.4 Flow Observations

4.4.1 Gas Flow Trend

The most noticeable trend shown by varying the occupation threshold is the connectivity of the pores which conduct gas flow. In other words, the size of the primary gas backbone decreases by increasing the occupation threshold. At a low occupation threshold, the network is more connected by which the gas flow can be divided into several flow paths near the minimum gas path. As observed in Figures 25 and 26, the size of the primary gas backbone highlighted in light green is significantly larger at lower occupation thresholds. This has consequences for the liquid flow since the larger the primary gas backbone, and the more space it takes up in the network, the less pores can be utilized for stable liquid flow.

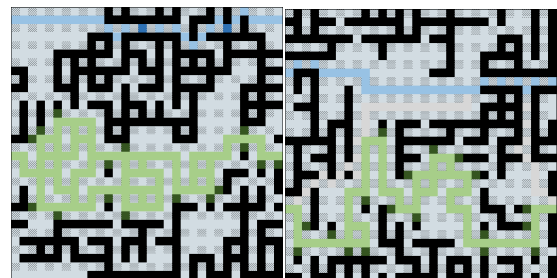


Figure 25 and 26: Flow for $p:0.48$ and $p:0.52$ of a 16×16 lattice

As stated in literature (King & Masihi, 2019) the percolation threshold is the occupation threshold at which one cluster arises across the network. This cluster spans in all directions thus allowing for a system where gas can be injected into any direction and the gas can flow across the network. The same was observed in this small scale pore network where gas was able to flow across the network in both directions (North to South, West to East) for the percolation threshold. However due to the restricted flow conditions with one inlet and one outlet on opposite sides of the lattice, the gas cannot always find a path across the lattice (see Figure 23). When the occupation threshold exceeds the percolation threshold, in most cases observed by the Excel method, gas could only flow in one direction. This can be problematic in cases where you cannot directly observe the network, and the gas inlet is in the direction

in which gas cannot flow. To ensure more gas flow, more outlets should be considered with a lattice that is at or below the percolation threshold.

Due to the lack of connectivity with a higher occupation threshold, it was often found that the gas takes a less direct and more tortuous path to reach the outlet. This is shown in Figure 26.

4.4.2 Water Flow Trend

As mentioned, the water flow across the lattice depends on the quantity, size and direction of the isolated clusters. These isolated clusters already occupy water and thus only require a driven velocity gradient to mobilize the water. The size and quantity of isolated cluster generally increases, the higher the occupation threshold and the less connected the network becomes. However, the direction of the isolated cluster, whether its longer in a certain direction, cannot be described as a function of the occupation threshold and remains random. For this reason and the randomness of percolation in the network, is it difficult to quantify linear behavior of the water conductivity as a function of the occupation threshold.

While creating the liquid flow path, we assumed that the liquid prefers the least amount of liquid bridges given that these liquid bridges take place in the smallest pore throats among the network. The consequence of this, is that the liquid path can be very tortuous. It could be that the liquid prefers a more direct path across the network with more liquid bridging.

4.4.3 Water and Gas Flow

While gas connectivity prefers a lower occupation threshold, water connectivity prefers the opposite. Therefore in order for both phases to find respective flow paths, flow is most ideal near the percolation threshold.

4.4.4 Problematic Flow Scenarios

In most cases, the liquid and gas will flow parallel across the lattice, where the liquid sometimes has to bridge a gas-filled pore throat of a dangling end. In the smaller pore space of 16 by 16 pores, the liquid and gas pathways were mostly found in close proximity to one another, especially for lower occupation thresholds. This is not the case with the larger pore space of 32 by 32 pores in which there is space between the gas and liquid pathways. In the vicinity of the primary gas backbone, it is more likely that the pores in the non-primary gas backbone, do have flowing gas. This space can be important in the stability of steady multiphase flow.



Figure 27: Flow for p : 0.485 of a 16x16 lattice



Figure 28: Flow for p : 0.490 of a 32x32 lattice

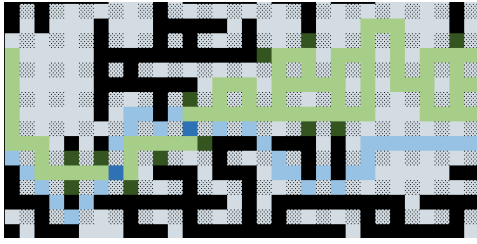


Figure 29: Crossflow of liquid and gas paths for $p: 0.490$ of a 16×16 lattice

Water flow where the liquid has to bridge a gas-filled pore that is part of the primary conducting gas backbone, can be problematic if one of the bridges fails. If it does fail and snap-off occurs, the newly made lamella can be directly mobilized by the gas and water gradient driven through the system. As a result, more lamellae can be created by recurring snap-off of the liquid bridges and lamella division by the mobilized lamella.

4.4.5 Additional Water Flow Paths

If the assumption that water will flow through the least amount of liquid bridges is false, the most likely route will be a more direct pathway and shorter path across the lattice. In Figure 30, two pathways are shown. Pathway 1 has fewer bridges and is less direct than pathway 2. However, pathway 2 has a more direct path and has bridges of very small size. This path is further away from the primary conducting backbone of gas and only transverses across dangling ends in the two liquid bridges.

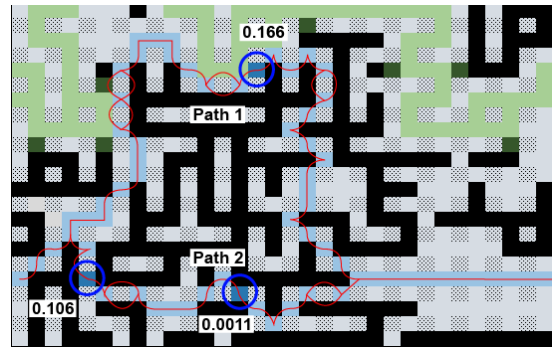


Figure 30: Optional water pathways across the small network of $p:0.485$

4.5 Observed Lamellae Generation Mechanisms

4.5.1 Leave Behind

Since we are considering that the gas has already established continuous flow across the medium, lamellae surrounding dangling ends can be formed by leave behind.

4.5.2 Lamella Division

Dangling ends can also form ideal conditions for lamella division. If a liquid-occupied pore throat separates two dangling ends, one can compute the pressure difference across the throat. This pressure difference is crucial to lamella creation and lamella division (Rossen & Gauglitz, 1990) (Rossen, 1996). In Figure 5, dangling ends span across most of the lattice and due to the wrap conditions of such lattice, several dangling ends of different regional pressures can be located relatively close to one another. This is also seen in Figure 6 where two sets of dangling ends are separated by one thin lamella.

5. Conclusions

The results of this study show that for a given percolating network near the percolation threshold, multiphase flow is heavily dependent on the feasibility of stable liquid bridging across gas-filled pore throats. Using percolation theory to form a connecting lattice, the connectivity of water and gas is most ideal near the percolation threshold. While gas flow is easier with a lower occupation threshold, water flow generally prefers a higher occupation threshold where there is a reduced connectivity of gas pathways. The water flow is difficult to describe as a function of the occupation threshold since the water flow can depend on the size, direction and quantity of isolated clusters formed by the percolating lattice in which water can move freely without resistance. However, regardless of how many isolated clusters are in a lattice at the percolation threshold, the water is likely to have to bridge a gas-filled pore throat.

Since liquid bridging is most favorable near the smallest possible pore throat along the water path, the water path took less direct forms of flow to cross the lattice and satisfy the assumed conditions (Cox, 2019). If this was not the case and the water flow took a more direct path, more liquid bridges are required.

To ensure steady multiphase flow without fluctuating pore occupancy, stable liquid bridging is required. Liquid bridging can be most problematic near the primary gas backbone. The primary conducting gas backbone decreases with size when the occupation threshold increases. The variable flowing gas velocity and pressure gradient in the primary backbone make for ideal conditions for lamella division once snap-off occurs (Rossen & Gauglitz, 1990). To ensure stability, the pore throats in the non-primary gas backbone that don't conduct gas flow, should be used for liquid bridging. When the percolating system is of a large size, it was observed that the primary gas backbone and the water path are located further from one another, allowing the water to flow in more ideal conditions.

Multiphase flow is also more feasible when more outlets are considered. In this investigation, we consider only one inlet and one outlet for each respective phase (based on the primary gas backbone and the water flow path). When more gas outlets are considered, the chance that the gas flows across the lattice is more likely as near the percolation threshold, one large cluster spans the system in all directions (King & Masihi, 2019). This was observed in the lattices at the percolation threshold in appendix A and B.

In the observed lattices, leave-behind was found as a product of the gas infiltrating the saturated pore space and stagnating as dangling ends. The surrounding lamellae can be explained by leave-behind. Furthermore, the lattices show ideal conditions for lamellae mobilization as lamella separated by dangling ends of different pressures, can be mobilized if the minimum pressure difference can be reached (Rossen & Gauglitz, 1990). This would ultimately be problematic in establishing multiphase flow.

6. Discussion

6.1 Modeling of the Gas and Water Paths

The condition for gas flow for the defined systems is limiting as shown by Figure 23 by the number of outlets and the position of the chosen outlet. If there are more outlets present is, there is a higher chance that gas flow will occur near the percolation threshold as at this threshold, one large cluster spans the entire system.

For each water flow, only a single path was devised with the given assumptions. If more pathways are highlighted with a different set of governing assumptions, several water flow paths can be weighed against one another.

6.2 Further Research and Considerations

6.2.1 Feasibility of Liquid Bridges

The possibility of multiphase flow in a 2D percolating network is dependent on the assumed feasibility of liquid bridges. However, in order to support the conclusions made, the validity of liquid bridges for the following settings requires confirmation:

- Liquid bridging across the primary gas backbone for variable flow rates of liquid and gas
- Liquid bridging across the non-primary gas backbone in presence of slow-moving and stagnated gas
- Consecutive liquid bridging of variable size

6.2.2 Volume Progression Through Liquid Bridges

Since we assume that the pressure gradient for both phases is constant and that the system is in steady state, we do not consider how the volume exactly advances through several liquid bridges. If we were to consider fluctuating flow rates throughout the lattice, variable capillary pressures have implications on the advancement of liquid volume across the lattice. Valencia et al. (2001) and Ahmadlouydarab et al. (2008) both state the importance of maintaining a constant flow rate in the stability of liquid bridging in a stationary case. Therefore, liquid accumulation should be avoided. The liquid volume that progresses through a large pore throat cannot always be accommodated by one of a significantly smaller size later in its path. If too much liquid volume is to cross a very narrow pore throat, the throat can be blocked by accumulated liquid and snap-off might occur. Therefore, it is likely that several liquid bridges might have to be utilized to transfer the same amount of liquid and maintain steady state. The two liquid bridges of path 2 in Figure 30 show this by first having a relative wide pore throat inhibiting the first liquid bridge followed by a much narrower pore throat for the second liquid bridge. There is an increased risk that accumulation happens at the second liquid bridge, which is not in line with the condition that is steady state. This is a consideration to keep in mind when considering a realistic system in unsteady state and variable pressure differences within the system.

6.2.3 Lamella Division Across Dangling Ends

The feasibility of multiphase flow relies on avoiding the formation of foam by any of the lamellae-generative mechanisms. Therefore, lamella division occurring near lamellae between consecutive dangling ends of different pressures can be problematic. The occurrence of this happening should be identified.

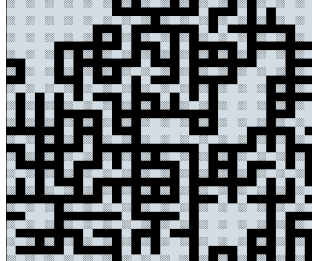

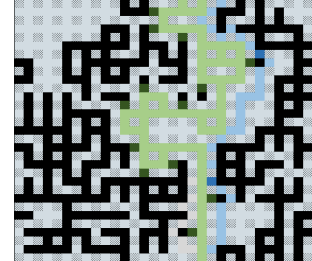
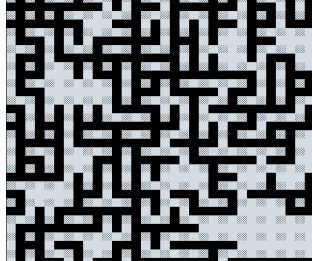


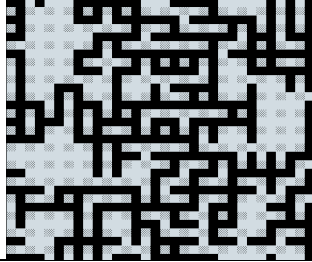
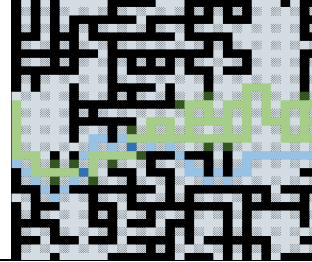
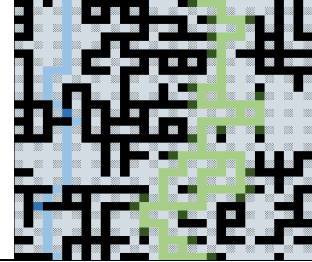
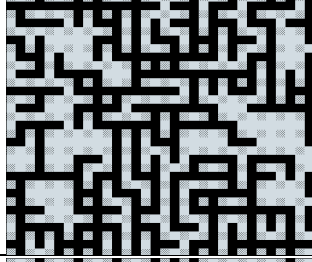


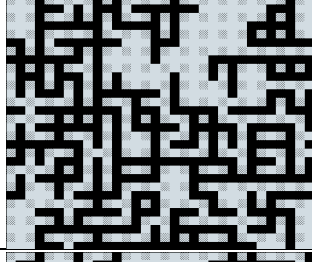
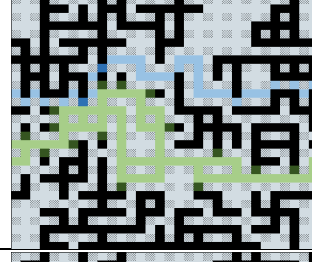



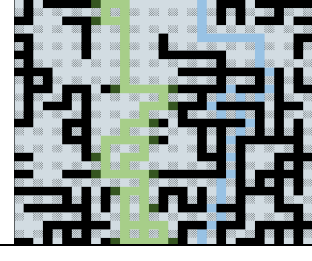
7. References

- Ahmadlouydarab, M., Azaiez, J., & Chen, Z. (2015). Dynamics of viscous liquid bridges inside microchannels subject to external oscillatory flow. *Physical Review E*, 91(2). doi: 10.1103/physreve.91.023002
- Broesch, D. J., & Frechette, J. (2012). From Concave to Convex: Capillary Bridges in Slit Pore Geometry. *Langmuir*, 28(44), 15548–15554. doi: 10.1021/la302942k
- Cox, S. (2019, Fall). Email communication.
- Fallahi, H., Zhang, J., Phan, H.-P., & Nguyen, N.-T. (2019). Flexible Microfluidics: Fundamentals, Recent Developments, and Applications. *Micromachines*, 10(12), 830. doi: 10.3390/mi10120830
- Hunt, A. G., Ewing, R. P., & Ghanbarian, B. (2014) *Percolation theory for flow in porous media*. Cham: Springer
- King, P. R., & Masihi, M. (2019). *Percolation theory in reservoir engineering*. London: World Scientific.
- Kirk, J. (2006). Dijkstra's Shortest Path Algorithm (<https://www.mathworks.com/matlabcentral/fileexchange/12850-dijkstra-s-shortest-path-algorithm>), MATLAB Central File Exchange.
- Kovscek, A., Tang, G.-Q., & Radke, C. (2007). Verification of Roof snap off as a foam-generation mechanism in porous media at steady state. *Colloids and Surfaces A: Physicochemical and Engineering Aspects*, 302(1-3), 251–260. doi: 10.1016/j.colsurfa.2007.02.035
- Kusumaatmaja, H., & Lipowsky, R. (2010). Equilibrium Morphologies and Effective Spring Constants of Capillary Bridges. *Langmuir*, 26(24), 18734–18741. doi: 10.1021/la102206d
- Lake, L., & Society of Petroleum Engineers of AIME. (2014). *Fundamentals of enhanced oil recovery* ([2nd ed.] ed.). Richardson, Tex.: Society of Petroleum Engineers.
- Larson, R., Scriven, L., & Davis, H. (1981). Percolation theory of two phase flow in porous media. *Chemical Engineering Science*, 36(1), 57–73. doi: 10.1016/0009-2509(81)80048-6
- Lifton, V. (2016). Microfluidics: An enabling screening technology for enhanced oil recovery (eor). *Lab on a Chip*, 16(10), 1777-96. doi:10.1039/c6lc00318d
- Moura, M., Flekkøy, E. G., Måløy, K. J., Schäfer, G., & Toussaint, R. (2019). Connectivity enhancement due to film flow in porous media. *Physical Review Fluids*, 4(9). doi: 10.1103/physrevfluids.4.094102
- Ransohoff, T., & Radke, C. (1988). Mechanisms of Foam Generation in Glass-Bead Packs. *SPE Reservoir Engineering*, 3(02), 573–585. doi: 10.2118/15441-pa
- Roof, J. (1970). Snap-Off of Oil Droplets in Water-Wet Pores. *Society of Petroleum Engineers Journal*, 10(01), 85–90. doi: 10.2118/2504-pa
- Rossen, W. R. (1990). Theory of mobilization pressure gradient of flowing foams in porous media. *Journal of Colloid and Interface Science*, 136(1), 1–16. doi: 10.1016/0021-9797(90)90074-x
- Rossen, W. R. (1996). Foams in Enhanced Oil Recovery. *Foams*, 413–464. doi: 10.1201/9780203755709-11

- Rossen, W. R. (2003). A critical review of Roof snap-off as a mechanism of steady-state foam generation in homogenous porous media. *Colloids and Surfaces A: Physicochemical and Engineering Aspects*, 225(1-3), 1-24. doi: 10.1016/s0927-7757(03)00309-1
- Rossen, W. R. (2008). Comment on "Verification of Roof snap-off as a foam-generation mechanism in porous media at steady state." *Colloids and Surfaces A: Physicochemical and Engineering Aspects*, 322(1-3), 261–269. doi: 10.1016/j.colsurfa.2008.02.034
- Rossen, W. R., & Gauglitz, P. A. (1990). Percolation theory of creation and mobilization of foams in porous media. *AIChE Journal*, 36(8), 1176–1188. doi: 10.1002/aic.690360807
- Rossen, W., & Duijn, C. V. (2004). Gravity segregation in steady-state horizontal flow in homogeneous reservoirs. *Journal of Petroleum Science and Engineering*, 43(1-2), 99–111. doi: 10.1016/j.petrol.2004.01.004
- Selyakov, V. I., & Kadet, V. V. (1996). *Percolation models for transport in porous media: with applications to reservoir engineering*. Dordrecht: Kluwer Academic Publishers.
- Shan, D., & Rossen, W. (2004). Optimal Injection Strategies for Foam IOR. *SPE Journal*, 9(02), 132–150. doi: 10.2118/88811-pa
- Valencia, A., Brinkmann, M., & Lipowsky, R. (2001). Liquid Bridges in Chemically Structured Slit Pores. *Langmuir*, 17(11), 3390–3399. doi: 10.1021/la001749q

Appendices

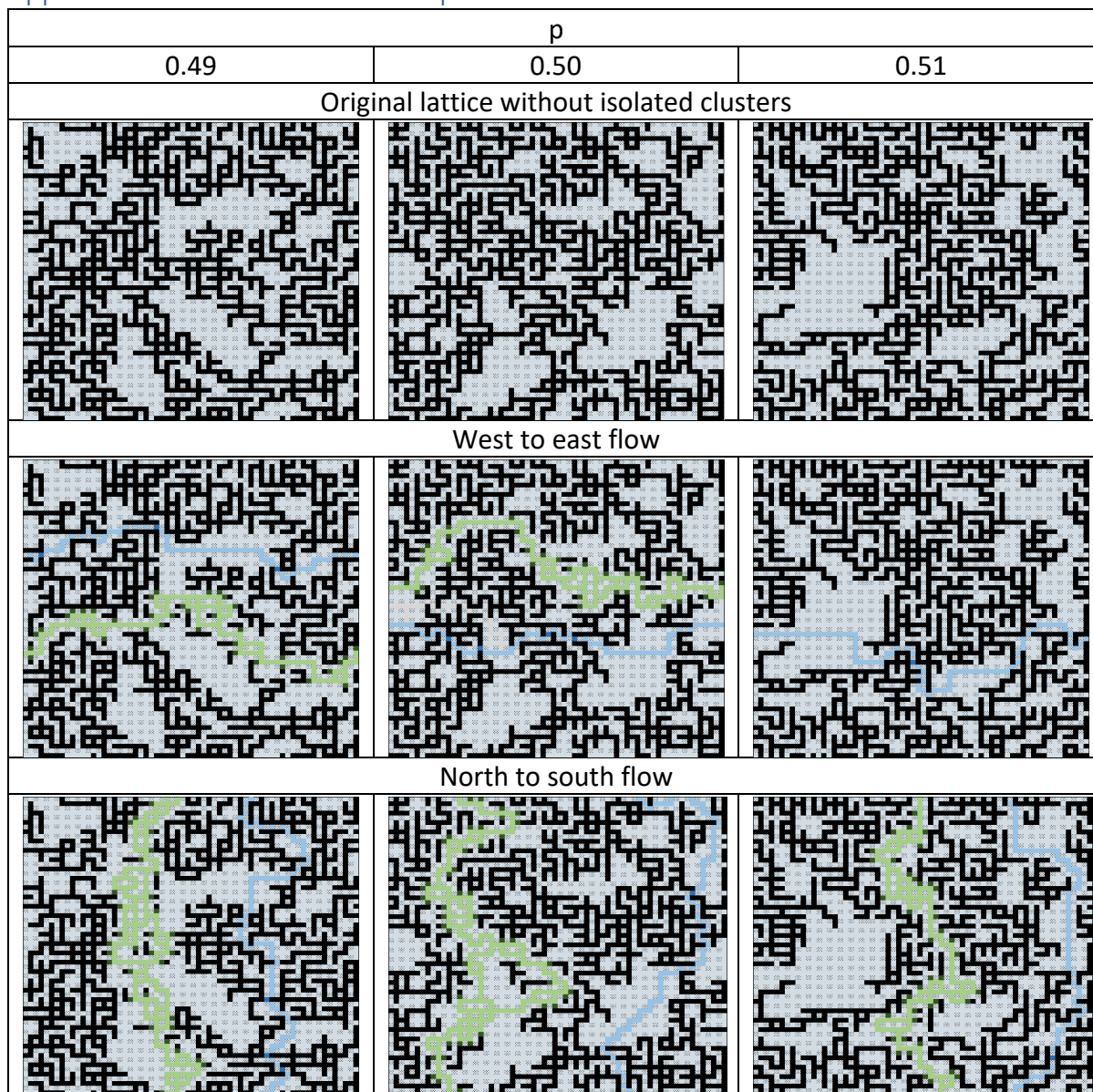
Appendix A – Excel Results: Pore Space 16 x 16

| p | Original lattice without isolated clusters | West to east flow | North to south flow |
|-------|---|--|---|
| 0.480 |  |  |  |
| 0.485 |  |  |  |
| 0.490 |  |  |  |
| 0.495 |  |  |  |
| 0.500 |  |  |  |
| 0.505 |  |  |  |

| | | | |
|-------|--|---|--|
| 0.510 |  |  |  |
| 0.515 |  |  |  |
| 0.520 |  |  |  |

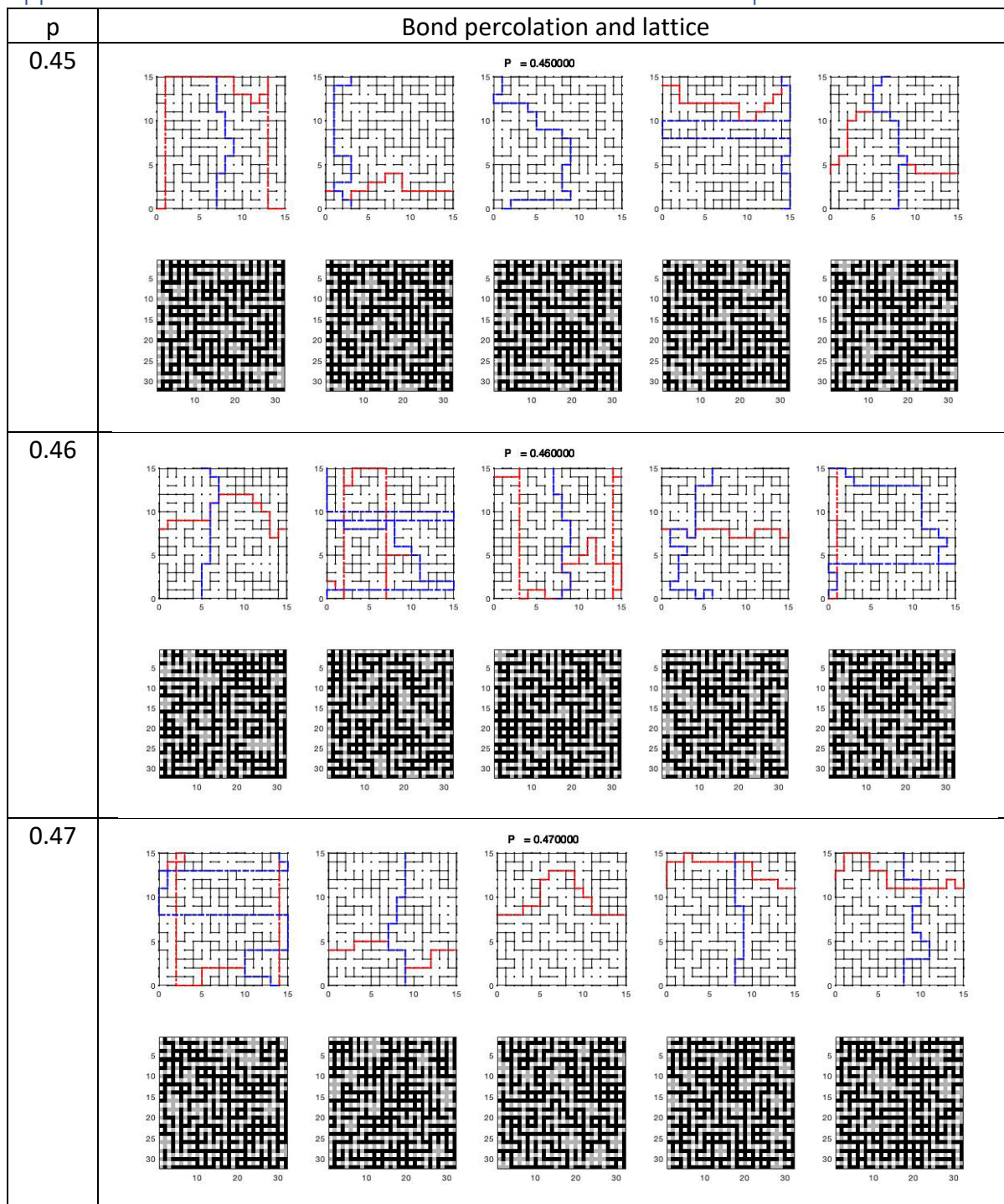
Note: Only the ends of the primary gas backbones are labeled.

Appendix B – Excel Results: Pore Space 32 x 32

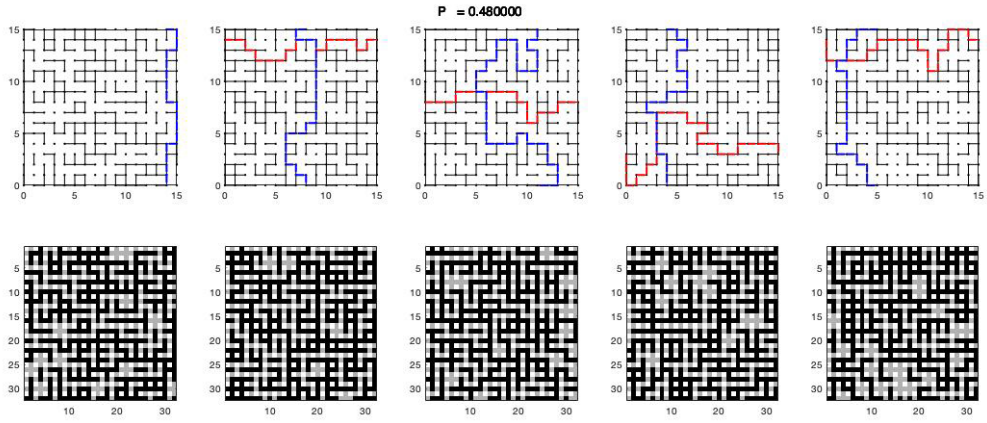


Note: Only the ends of the primary gas backbones are labeled.

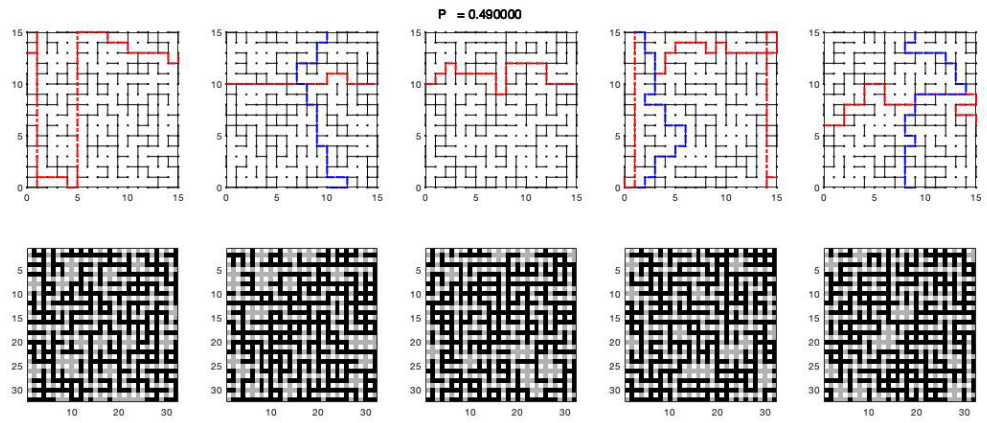
Appendix C – MATLAB Results: Bond Percolation and Lattice for p:0.45-0.55



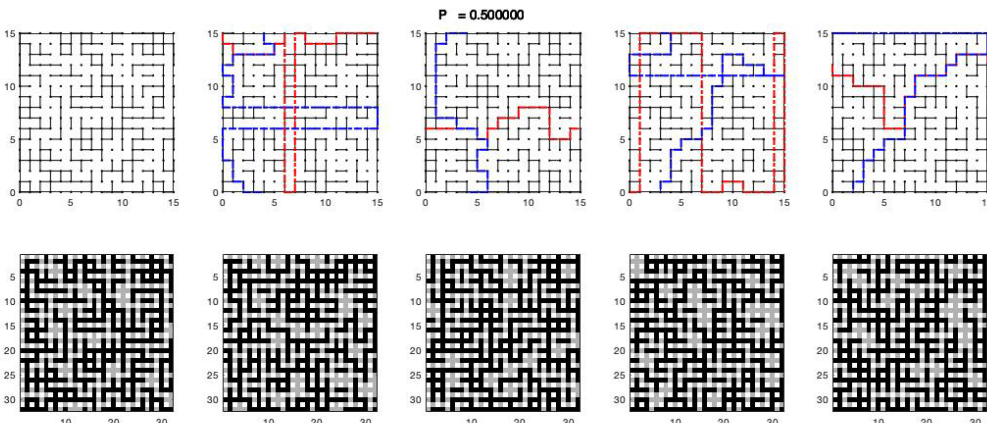
0.48



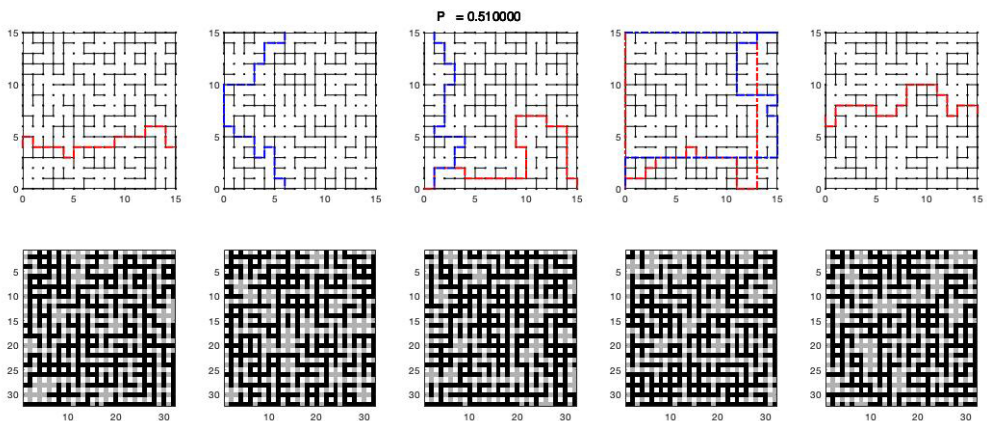
0.49

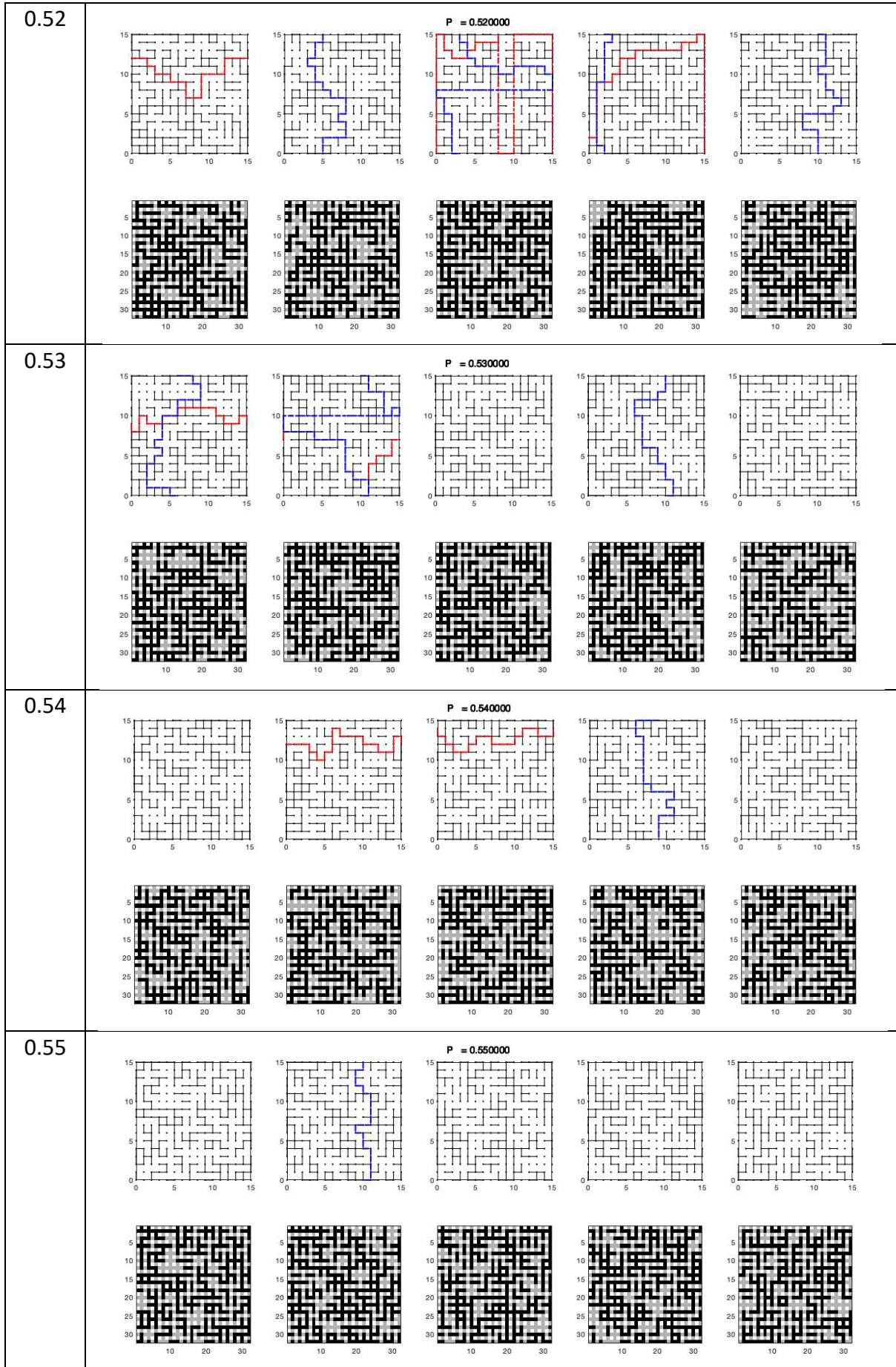


0.50



0.51





Appendix D – MATLAB Script: Bond Percolation and Lattice for p:0.45-0.55

```

%% Parameters
L=32; %for 16x16 pore space
O=5; %#of iterations
Pbeg=0.45; %Beginning value occupation threshold
PI=0.01; %Steps of occupation threshold
Pend=0.55; %End value occupation threshold

%% Simplifications for later
L1=L/2;
PS=L*L/4;
L2=L*L;
PG=round(((Pend-Pbeg)./PI)+1);
Pc=Pbeg:PI:Pend;
MDF=ones(O,PG);

%% For Loop Iterations and P
for P=Pbeg:PI:Pend
str = sprintf('Pc = %f', P);
Q=round((P-Pbeg)/PI)+1;
figure;
for o=1:O

%% Making of the Percolation Lattice
U=rand(L,L);

%% Bond Percolation Lattice

A=U;
A(2:2:end,2:2:end)=0;
A(1:2:end,1:2:end)=0;
for i=2:2:L
    A(1:2:L-1,i)=A(1:2:L-1,i)-P;
end
for i=1:2:L-1
    A(2:2:L,i)=A(2:2:L,i)-P;
end
A(A<=0)=0;
A(1:2:end,1:2:end)=0;
No=length(nonzeros(A(A>0)));
Lno=No*2;
S1=zeros(1,Lno);
T1=zeros(1,Lno);
S2=zeros(1,Lno);
T2=zeros(1,Lno);
S3=zeros(1,Lno);
T3=zeros(1,Lno);
S4=zeros(1,Lno);
T4=zeros(1,Lno);
for i=2:2:L
    for j=2:2:L
        A(i,j)=(j/2)+((i-2)/2)*(L/2);
    end
end

%%inner nodes top-bot
for k=(3:2:L-1)
    for l=(2:2:L)
        m1=(k+l-4)+((k-3)/2)*L;
        m2=(k+l-3)+((k-3)/2)*L;
        if A(k,l)>0

```

```

        S1(1,m1)=A(k-1,1);
        S1(1,m2)=A(k+1,1);
        T1(1,m1)=A(k+1,1);
        T1(1,m2)=A(k-1,1);
    end
end
end
S1( :, ~any(S1,1) ) = [];
T1( :, ~any(T1,1) ) = [];

%inner nodes left-right
for m=(2:2:L)
    for n=(3:2:L-1)
        m3=(m+n-4)+((m-2)/2)*L;
        m4=(m+n-3)+((m-2)/2)*L;
        if A(m,n)>0
            S2(1,m3)=A(m,n-1);
            S2(1,m4)=A(m,n+1);
            T2(1,m3)=A(m,n+1);
            T2(1,m4)=A(m,n-1);
        end
    end
end
S2( :, ~any(S2,1) ) = [];
T2( :, ~any(T2,1) ) = [];

%Top boundary conditions
for q=(2:2:L)
    m5=q-1;
    m6=q;
    if A(1,q)>0
        S3(1,m5)=A(2,q);
        S3(1,m6)=A(L,q);
        T3(1,m5)=A(L,q);
        T3(1,m6)=A(2,q);
    end
end
S3( :, ~any(S3,1) ) = [];
T3( :, ~any(T3,1) ) = [];

%Left boundary conditions
for r=(2:2:L)
    m7=r-1;
    m8=r;
    if A(r,1)>0
        S4(1,m7)=A(r,2);
        S4(1,m8)=A(r,L);
        T4(1,m7)=A(r,L);
        T4(1,m8)=A(r,2);
    end
end
S4( :, ~any(S4,1) ) = [];
T4( :, ~any(T4,1) ) = [];

S=[S1,S2];
T=[T1,T2];
SLR=[S1,S2,S3];
TLR=[T1,T2,T3];
STB=[S1,S2,S4];
TTB=[T1,T2,T4];

```

```

%% System Coordinates & Nodes and Segments Definition

```



```

NoNodes =1:PS;
X=[(0:15), (0:15), (0:15), (0:15), (0:15), (0:15), (0:15), (0:15),
(0:15), (0:15), (0:15), (0:15), (0:15), (0:15), (0:15), (0:15)];
Y=[15*ones(1,16), 14*ones(1,16), 13*ones(1,16), 12*ones(1,16),
11*ones(1,16), 10*ones(1,16), 9*ones(1,16), 8*ones(1,16), 7*ones(1,16),
6*ones(1,16), 5*ones(1,16), 4*ones(1,16), 3*ones(1,16), 2*ones(1,16),
ones(1,16), zeros(1,16)];
nodes = [NoNodes; X ; Y]';
segments = [(1:numel(S)) ; S ; T]';
segmentsLR = [(1:numel(SLR)) ; SLR ; TLR]';
segmentsTB = [(1:numel(STB)) ; STB ; TTB]';

%% Calculating Shortest Path and Plotting
subplot(2,0,0); sgtitle(str); plot(nodes(:,2), nodes(:,3),'k. '); hold on;
for s = 1:numel(S)

plot(nodes(segments(s,2:3)',2),nodes(segments(s,2:3)',3),'k ');
end

%Left to Right Condition
Nbeg1=zeros(1,(L/2));
Nend1=zeros(1,(L/2));
for z=2:2:L
if A(z,1)>0
Nbeg1(z/2)=A(z,2);
Nend1(z/2)=Nbeg1(z/2)+(L/2)-1;
end
end
Nbeg1( :, ~any(Nbeg1,1) ) = [];
Nend1( :, ~any(Nend1,1) ) = [];

d1=[zeros(1,length(Nbeg1))]' ;
for y=1:1:length(Nbeg1)
[d1(y), gh] = dijkstra(nodes, segmentsLR, Nbeg1(y), Nend1(y));
for dd=1:length(gh)-1
if abs((gh(dd+1)-gh(dd)))==15
d1(y)=d1(y)-14;
end
if abs((gh(dd+1)-gh(dd)))==240
d1(y)=d1(y)-14;
end
end
end
[ minpath,b] = min(d1(d1>15));
[d2, p2] = dijkstra(nodes, segmentsLR, Nbeg1(b), Nend1(b));
minpath(~isfinite(minpath))=0;
for n2 = 2:length(p2)
plot(nodes(p2(n2-1:n2),2),nodes(p2(n2-1:n2),3),'r-
.', 'linewidth',2);
end

%Top to Bottom Condition
Nbeg2=zeros(1,(L/2));
Nend2=zeros(1,(L/2));
for z=2:2:L
if A(1,z)>0
Nbeg2(z/2)=A(2,z);
Nend2(z/2)=(L*L/4)-((L/2)-Nbeg2(z/2));
end
end
Nbeg2( :, ~any(Nbeg2,1) ) = [];
Nend2( :, ~any(Nend2,1) ) = [];

```

```

d3=[zeros(1,length(Nbeg2))]' ;
for g=1:length(Nbeg2)
    [d3(g), p] = dijkstra(nodes, segmentsTB, Nbeg2(g), Nend2(g));
    for aa=1:length(p)-1
        if abs((p(aa+1)-p(aa)))==15
            d3(g)=d3(g)-14;
        end
        if abs((p(aa+1)-p(aa)))==240
            d3(g)=d3(g)-14;
        end
    end
end
[minpath2,a] = min(d3);
[d4, p3] = dijkstra(nodes, segmentsTB, Nbeg2(a), Nend2(a));
minpath2(~isfinite(minpath2))=0;
for n3 = 2:length(p3)
    plot(nodes(p3(n3-1:n3),2),nodes(p3(n3-1:n3),3), 'b-
.', 'linewidth', 2);
end
hold off;

%% MD Calculation
MD=[minpath;minpath2] ;

if MD==[0;0]
    MDF(o,Q)=0;
else
    MDF(o,Q)= min(MD);
end

%% Imagesc
U(2:2:end,2:2:end)=0;
U(1:2:end,1:2:end)=0;
for i=2:2:L
    U(1:2:L-1,i)=U(1:2:L-1,i)-P;
end
for i=1:2:L-1
    U(2:2:L,i)=U(2:2:L,i)-P;
end
U(U<=0)=0;
U(1:2:end,1:2:end)=0;

%Pore Bodies
f = ones(3); %filter
U2 = [U(:, :), U(:, 1); U(1, :), 0];
U3 = conv2(U2, f, 'same');
for j=2:2:L
    for k=2:2:L;
        U(j,k) = U3(j,k);
        if U(j,k)>0;
            U(j,k)=0.1;
        end
    end
end

%Pore Pillars
U(1:2:end,1:2:end)=1;

for v=1:L
    for d=1:L

```

```
        if U(v,d)>0 && U(v,d)<1
            U(v,d)=0.5;
        end
    end
end

%Colors & Graph
Black = [0 0 0]; %Open Pores
Gray = [0.7 0.7 0.7]; %Closed Pores
White = [1 1 1]; %Pillars
My_Map = [Gray; Black; White];
colormap(My_Map); caxis([0 0.5]); subplot(2,0,0+o); imagesc(U)
end
end
```

Appendix E – MATLAB Script: Percolation Statistics for p:0.40-0.60

```

%% Parameters
L=32; %for 16x16 pore space
O=100; %#of iterations
Pbeg=0.40; %Beginning value occupation threshold
PI=0.01; %Steps of occupation threshold
Pend=0.60; %End value occupation threshold

%% Simplifications for later
L1=L/2;
PS=L*L/4;
L2=L*L;
PG=round( ( (Pend-Pbeg) ./PI)+1);
PGMin=2*PG;
Pc=Pbeg:PI:Pend;
MDF=ones(O,PG);
MDTBRL=ones(O,PGMin);
MDFF=ones(O,PG);

%% For Loop Iterations and P
for P=Pbeg:PI:Pend
Q=round( (P-Pbeg)/PI)+1;
for o=1:O

%% Making of the Percolating Lattice
A=rand(L,L);

%% Bond Percolating Lattice
A(2:2:end,2:2:end)=0;
A(1:2:end,1:2:end)=0;
for i=2:2:L
    A(1:2:L-1,i)=A(1:2:L-1,i)-P;
end
for i=1:2:L-1
    A(2:2:L,i)=A(2:2:L,i)-P;
end
A(A<=0)=0;
A(1:2:end,1:2:end)=0;
No=length(nonzeros(A(A>0)));
Lno=No*2;
S1=zeros(1,Lno);
T1=zeros(1,Lno);
S2=zeros(1,Lno);
T2=zeros(1,Lno);
S3=zeros(1,Lno);
T3=zeros(1,Lno);
S4=zeros(1,Lno);
T4=zeros(1,Lno);
for i=2:2:L
    for j=2:2:L
        A(i,j)=(j/2)+((i-2)/2)*(L/2);
    end
end

%%inner nodes top-bot
for k=(3:2:L-1)
    for l=(2:2:L)
        m1=(k+l-4)+((k-3)/2)*L;
        m2=(k+l-3)+((k-3)/2)*L;
        if A(k,l)>0
            S1(1,m1)=A(k-1,l);
        end
    end
end

```

```

        S1(1,m2)=A(k+1,1);
        T1(1,m1)=A(k+1,1);
        T1(1,m2)=A(k-1,1);
    end
end
end
S1( :, ~any(S1,1) ) = [];
T1( :, ~any(T1,1) ) = [];

%inner nodes left-right
for m=(2:2:L)
    for n=(3:2:L-1)
        m3=(m+n-4)+((m-2)/2)*L;
        m4=(m+n-3)+((m-2)/2)*L;
        if A(m,n)>0
            S2(1,m3)=A(m,n-1);
            S2(1,m4)=A(m,n+1);
            T2(1,m3)=A(m,n+1);
            T2(1,m4)=A(m,n-1);
        end
    end
end
S2( :, ~any(S2,1) ) = [];
T2( :, ~any(T2,1) ) = [];

for q=(2:2:L)
    m5=q-1;
    m6=q;
    if A(1,q)>0 %Top boundary conditions
        S3(1,m5)=A(2,q);
        S3(1,m6)=A(L,q);
        T3(1,m5)=A(L,q);
        T3(1,m6)=A(2,q);
    end
    if A(q,1)>0 %Left boundary conditions
        S4(1,m5)=A(q,2);
        S4(1,m6)=A(q,L);
        T4(1,m5)=A(q,L);
        T4(1,m6)=A(q,2);
    end
end
S3( :, ~any(S3,1) ) = [];
T3( :, ~any(T3,1) ) = [];
S4( :, ~any(S4,1) ) = [];
T4( :, ~any(T4,1) ) = [];

S=[S1,S2];
T=[T1,T2];
SLR=[S1,S2,S3];
TLR=[T1,T2,T3];
STB=[S1,S2,S4];
TTB=[T1,T2,T4];

%% System Coordinates & Nodes and Segments Definition
NoNodes =1:PS;
X=[(0:15), (0:15), (0:15), (0:15), (0:15), (0:15), (0:15), (0:15),
(0:15), (0:15), (0:15), (0:15), (0:15), (0:15), (0:15), (0:15)];
Y=[15*ones(1,16), 14*ones(1,16), 13*ones(1,16), 12*ones(1,16),
11*ones(1,16), 10*ones(1,16), 9*ones(1,16), 8*ones(1,16), 7*ones(1,16),
6*ones(1,16), 5*ones(1,16), 4*ones(1,16), 3*ones(1,16), 2*ones(1,16),
ones(1,16), zeros(1,16)];
nodes = [NoNodes; X ; Y]';

```

```

segments = [(1:numel(S)) ; S ; T]';
segmentsLR = [(1:numel(SLR)) ; SLR ; TLR]';
segmentsTB = [(1:numel(STB)) ; STB ; TTB]';

%% Calculating Shortest Path and Plotting
%Left to Right Condition
Nbeg1=zeros(1,(L/2));
Nend1=zeros(1,(L/2));
for z=2:2:L
    if A(z,1)>0
        Nbeg1(z/2)=A(z,2);
        Nend1(z/2)=Nbeg1(z/2)+(L/2)-1;
    end
end
Nbeg1( :, ~any(Nbeg1,1) ) = [];
Nend1( :, ~any(Nend1,1) ) = [];

d1=[zeros(1,length(Nbeg1))]' ;
for y=1:1:length(Nbeg1)
    [d1(y), gh] = dijkstra(nodes, segmentsLR, Nbeg1(y), Nend1(y));
    for dd=1:length(gh)-1
        if abs((gh(dd+1)-gh(dd)))==15
            d1(y)=d1(y)-14;
        end
        if abs((gh(dd+1)-gh(dd)))==240
            d1(y)=d1(y)-14;
        end
    end
end
[minpath,b] = min(d1(d1>15));
[d2, p2] = dijkstra(nodes, segmentsLR, Nbeg1(b), Nend1(b));
minpath(~isfinite(minpath))=0;

%Top to Bottom Condition
Nbeg2=zeros(1,(L/2));
Nend2=zeros(1,(L/2));
for z=2:2:L
    if A(1,z)>0
        Nbeg2(z/2)=A(2,z);
        Nend2(z/2)=(L*L/4)-((L/2)-Nbeg2(z/2));
    end
end
Nbeg2( :, ~any(Nbeg2,1) ) = [];
Nend2( :, ~any(Nend2,1) ) = [];

d3=[zeros(1,length(Nbeg2))]' ;
for g=1:1:length(Nbeg2)
    [d3(g), p] = dijkstra(nodes, segmentsTB, Nbeg2(g), Nend2(g));
    for aa=1:length(p)-1
        if abs((p(aa+1)-p(aa)))==15
            d3(g)=d3(g)-14;
        end
        if abs((p(aa+1)-p(aa)))==240
            d3(g)=d3(g)-14;
        end
    end
end
% d3(~isfinite(d3))=0;
[minpath2,a] = min(d3);
[d4, p3] = dijkstra(nodes, segmentsTB, Nbeg2(a), Nend2(a));
minpath2(~isfinite(minpath2))=0;

```

```

%% MD Calculation
MD=[minpath;minpath2];
Q1=2*Q-1;
Q2=2*Q;
MDTBRL(o,Q1)=minpath;
MDTBRL(o,Q2)=minpath2;

if MD==[0;0]
    MDF(o,Q)=0;
elseif MD(1,1)==0 && MD(2,1)>0
    MDF(o,Q)= MD(2,1);
elseif MD(2,1)==0 && MD(1,1)>0
    MDF(o,Q)= MD(1,1);
elseif MD(1,1)>0 && MD(2,1)>0
    MDF(o,Q)= min(MD);
end

if minpath>0 && minpath2>0
    MDFF(o,Q)=1;
else
    MDFF(o,Q)=0;
end

end %Number of Iterations O
end %Occupation threshold P

%% Statistics

MinDistance=ones(1,PG);
NumberFlow=ones(1,PG);
NumberLRFlow=ones(1,PG);
NumberTBFlow=ones(1,PG);
NumberBothFlow=ones(1,PG);

for h = 1:PG
    MinDistance(h) = mean(MDF((MDF(:, h) ~= 0), h));
    NumberFlow(h)=nnz(MDF(:,h)>0);
    Q3 = 2*h-1;
    NumberLRFlow(h)=nnz(MDTBRL(:,Q3)>0);
    Q4 = 2*h;
    NumberTBFlow(h)=nnz(MDTBRL(:,Q4)>0);
    NumberBothFlow(h)=nnz(MDFF(:,h)>0);
end

%% Plot Statistics
figure;
subplot (1,2,1); plot(Pc,MinDistance);
title('Flow top-bot, left-right');
xlabel('Occupation threshold');
ylabel('Minimum Distance');

subplot (1,2,2);
plot(Pc,NumberFlow); hold on;
plot(Pc, NumberLRFlow);
plot(Pc, NumberTBFlow);
plot(Pc, NumberBothFlow);
legend('No. of Flowing Systems', 'Horizontal Flow', 'Vertical Flow',
'Horizontal And Vertical Flow')

```

```
str2 = sprintf('Number of flowing systems out of 100 Iterations');  
title('Number of flowing systems'); xlabel('Occupation threshold');  
ylabel(str2);  
str = sprintf('Percolating Systems');  
sgtitle(str);
```


Appendix F – MATLAB Script: Dijkstra's Shortest Path Algorithm

```
function [dist,path] = dijkstra(nodes,segments,start_id,finish_id)
%DIJKSTRA Calculates the shortest distance and path between points on a
map
% using Dijkstra's Shortest Path Algorithm
%
% [DIST, PATH] = DIJKSTRA(NODES, SEGMENTS, SID, FID)
% Calculates the shortest distance and path between start and finish
nodes SID and FID
%
% [DIST, PATH] = DIJKSTRA(NODES, SEGMENTS, SID)
% Calculates the shortest distances and paths from the starting node
SID to all
% other nodes in the map
%
% Note:
% DIJKSTRA is set up so that an example is created if no inputs are
provided,
% but ignores the example and just processes the inputs if they are
given.
%
% Inputs:
% NODES should be an Nx3 or Nx4 matrix with the format [ID X Y] or
[ID X Y Z]
% where ID is an integer, and X, Y, Z are cartesian position
coordinates)
% SEGMENTS should be an Mx3 matrix with the format [ID N1 N2]
% where ID is an integer, and N1, N2 correspond to node IDs from
NODES list
% such that there is an [undirected] edge/segment between node N1
and node N2
% SID should be an integer in the node ID list corresponding with the
starting node
% FID (optional) should be an integer in the node ID list
corresponding with the finish
%
% Outputs:
% DIST is the shortest Euclidean distance
% If FID was specified, DIST will be a 1x1 double representing the
shortest
% Euclidean distance between SID and FID along the map segments.
DIST will have
% a value of INF if there are no segments connecting SID and FID.
% If FID was not specified, DIST will be a 1xN vector representing
the shortest
% Euclidean distance between SID and all other nodes on the map.
DIST will have
% a value of INF for any nodes that cannot be reached along
segments of the map.
% PATH is a list of nodes containing the shortest route
% If FID was specified, PATH will be a 1xP vector of node IDs from
SID to FID.
% NAN will be returned if there are no segments connecting SID to
FID.
% If FID was not specified, PATH will be a 1xN cell of vectors
representing the
% shortest route from SID to all other nodes on the map. PATH
will have a value
% of NAN for any nodes that cannot be reached along the segments
of the map.
%
```

```

if (nargin < 3) % SETUP
    num_nodes = 40; L = 100; max_seg_length = 30; ids = (1:num_nodes)';
    nodes = [ids L*rand(num_nodes,2)]; % create random nodes
    h = figure; plot(nodes(:,2),nodes(:,3),'k.') % plot the nodes
    text(nodes(num_nodes,2),nodes(num_nodes,3),...
        [' ' num2str(ids(num_nodes))], 'Color','b', 'FontWeight','b')
    hold on
    num_segs = 0; segments = zeros(num_nodes*(num_nodes-1)/2,3);
    for i = 1:num_nodes-1 % create edges between some of the nodes
        text(nodes(i,2),nodes(i,3),[' '
num2str(ids(i))], 'Color','b', 'FontWeight','b')
        for j = i+1:num_nodes
            d = sqrt(sum((nodes(i,2:3) - nodes(j,2:3)).^2));
            if and(d < max_seg_length,rand < 0.6)
                plot([nodes(i,2) nodes(j,2)], [nodes(i,3) nodes(j,3)], 'k.-
')
                    % add this link to the segments list
                    num_segs = num_segs + 1;
                    segments(num_segs,:) = [num_segs nodes(i,1) nodes(j,1)];
            end
        end
    end
    segments(num_segs+1:num_nodes*(num_nodes-1)/2,:) = [];
    axis([0 L 0 L])
    % Calculate Shortest Path Using Dijkstra's Algorithm
    % Get random starting/ending nodes, compute the shortest distance and
    path.
    start_id = ceil(num_nodes*rand); disp(['start id = '
num2str(start_id)]);
    finish_id = ceil(num_nodes*rand); disp(['finish id = '
num2str(finish_id)]);
    [distance,path] = dijkstra(nodes,segments,start_id,finish_id);
    disp(['distance = ' num2str(distance)]); disp(['path = ['
num2str(path) ']]);
    % If a Shortest Path exists, Plot it on the Map.
    figure(h)
    for k = 2:length(path)
        m = find(nodes(:,1) == path(k-1));
        n = find(nodes(:,1) == path(k));
        plot([nodes(m,2) nodes(n,2)], [nodes(m,3) nodes(n,3)], 'ro-
', 'LineWidth', 2);
    end
    title(['Shortest Distance from ' num2str(start_id) ' to ' ...
num2str(finish_id) ' = ' num2str(distance)])
    hold off
else %-----
-----
    % MAIN FUNCTION - DIJKSTRA'S ALGORITHM

    % initializations
    node_ids = nodes(:,1);
    [num_map_pts,cols] = size(nodes);
    table = sparse(num_map_pts,2);
    shortest_distance = Inf(num_map_pts,1);
    settled = zeros(num_map_pts,1);
    path = num2cell(NaN(num_map_pts,1));
    col = 2;
    pidx = find(start_id == node_ids);
    shortest_distance(pidx) = 0;
    table(pidx,col) = 0;
    settled(pidx) = 1;

```

```

path(pidx) = {start_id};
if (nargin < 4) % compute shortest path for all nodes
    while_cmd = 'sum(~settled) > 0';
else % terminate algorithm early
    while_cmd = 'settled(zz) == 0';
    zz = find(finish_id == node_ids);
end
while eval(while_cmd)
    % update the table
    table(:,col-1) = table(:,col);
    table(pidx,col) = 0;
    % find neighboring nodes in the segments list
    neighbor_ids = [segments(node_ids(pidx) == segments(:,2),3);
        segments(node_ids(pidx) == segments(:,3),2)];
    % calculate the distances to the neighboring nodes and keep track
of the paths
    for k = 1:length(neighbor_ids)
        cidx = find(neighbor_ids(k) == node_ids);
        if ~settled(cidx)
            d = sqrt(sum((nodes(pidx,2:cols) -
nodes(cidx,2:cols)).^2));
            if (table(cidx,col-1) == 0) || ...
                (table(cidx,col-1) > (table(pidx,col-1) + d))
                table(cidx,col) = table(pidx,col-1) + d;
                tmp_path = path(pidx);
                path(cidx) = {[tmp_path{1} neighbor_ids(k)]};
            else
                table(cidx,col) = table(cidx,col-1);
            end
        end
    end
    % find the minimum non-zero value in the table and save it
    nidx = find(table(:,col));
    ndx = find(table(nidx,col) == min(table(nidx,col)));
    if isempty(ndx)
        break
    else
        pidx = nidx(ndx(1));
        shortest_distance(pidx) = table(pidx,col);
        settled(pidx) = 1;
    end
end
if (nargin < 4) % return the distance and path arrays for all of the
nodes
    dist = shortest_distance';
    path = path';
else % return the distance and path for the ending node
    dist = shortest_distance(zz);
    path = path(zz);
    path = path{1};
end
end

```